12-2015

Evaluation of Fuel Flow Measurement Uncertainty in a Turbine Engine Test Cell

Paul Andrew Wright
University of Tennessee - Knoxville, pwrigh15@vols.utk.edu

To the Graduate Council:

I am submitting herewith a thesis written by Paul Andrew Wright entitled "Evaluation of Fuel Flow Measurement Uncertainty in a Turbine Engine Test Cell." I have examined the final electronic copy of this thesis for form and content and recommend that it be accepted in partial fulfillment of the requirements for the degree of Master of Science, with a major in Mechanical Engineering.

Trevor Moeller, Major Professor

We have read this thesis and recommend its acceptance:

James Simonton, Ahmad Vikili

Accepted for the Council:
Carolyn R. Hodges

Vice Provost and Dean of the Graduate School

(Original signatures are on file with official student records.)

Evaluation of Fuel Flow Measurement Uncertainty in a Turbine Engine Test Cell

A Thesis Presented for the

Master of Science

Degree

The University of Tennessee, Knoxville

Paul Andrew Wright

December 2015

DEDICATION

I would like to dedicate this work to my wife, Jordan, and my daughter, Eleanor, for the constant patience and support that they provided throughout my Master's degree program and especially during the preparation of this thesis. I would also like to dedicate this to my parents, Roger and Mary, who taught me a strong work ethic and always emphasized the importance of education and the idea that we should never stop learning.

ACKNOWLEDGEMENTS

I would like to thank all those that helped and provided their support during the preparation of this thesis. A special thank you is due to Dr. Rob McAmis for introducing me to the subject of measurement uncertainty and giving me this special project and to Mr. Alvis Turrentine who provided a great deal of help throughout in understanding the importance and principles of measurement uncertainty. I would also like to thank many of my coworkers who helped me navigate the Master's degree waters and answered my countless questions about how the process works. I would also like to thank the chair of my thesis committee, Dr. Trevor Moeller, and thesis committee members, Dr. James Simonton and Dr. Ahmad Vakili, for helping me through the thesis process and providing their technical expertise. I would also like to thank Arnold Air Force Base for providing time and resources to complete this thesis.

ABSTRACT

The evaluation of measurement uncertainty is an essential part of measurement and data analysis. Measurement uncertainty is itself a measure of the "goodness" of the measured data and helps the analyst to make decisions based on the data. In the turbine engine testing world, accurate measurement of fuel flow is critical. Specific fuel consumption is a combination of thrust and fuel flow and is used to calculate the allowable payload and range of an aircraft as well as the cruising speed. Naturally, test customers (engine manufacturers, aircraft designers, and operators) are very sensitive to the accuracy of fuel flow measurement. This thesis presents a statistically defensible methodology for determining the uncertainty of fuel flow measurement in a turbine engine test cell.

Fuel flow in most turbine engine test applications is measured using a volumetric turbine flowmeter. The mass flow rate of the fuel flow is calculated using the SAE ARP 4990 standard. The ARP 4990 method of fuel flow calculation is complicated and involves many parameters. An analysis of the influence coefficients for each of the input parameters was performed and found that four main parameters have a significant impact on fuel flow uncertainty: flowmeter frequency, flowmeter calibration, fuel operating temperature, and relative density at a chosen reference temperature. A method was developed for deriving a statistically defensible estimate of the uncertainty for each of the elemental error sources. The elemental uncertainties were then propagated to

the result using both the Taylor's Series method and the Monte Carlo method, which yielded nearly identical results.

The method presented herein will aid in the evaluation of fuel flow uncertainty at AEDC. Compared to historical practices, this method results in a significant reduction in total fuel flow uncertainty and a much higher degree of statistical defensibility.

TABLE OF CONTENTS

LIST OF TABLES

LIST OF FIGURES

NOMENCLATURE

β	True systematic error
Δ	Difference between redundant measurements
$\bar{\Delta}$	Average difference between redundant measurements
ϵ	True random error
δ	True total error
ν	Degrees of freedom
σ	True standard deviation
σ^2	True variance
θ	Absolute influence coefficient
θ'	Relative influence coefficient
b	Systematic uncertainty
k	Student's t-value for the desired coverage interval using the ISO GUM uncertainty method
MCM	Monte Carlo method
r	Calculation result
r_{true}	True value of the result

s	Random uncertainty
t_{95}	Student's t-value for the 95% confidence interval
TSM	Taylor's Series method
u	Combined (total) uncertainty at the one-standard deviation level
U_{95}	Expanded uncertainty at the 95% confidence interval derived using the ASME method
U_{ADD}	Expanded uncertainty using the additive uncertainty method
U_{ISO}	Expanded uncertainty at the 95% confidence interval derived using the ISO GUM method
U_{RSS}	Expanded uncertainty using the root-sum-square method
x_{true}	True value of an independent measurement, x
$\overline{X}$	Average of a population of measurements
y_{true}	True value of an independent measurement, y

1.0 INTRODUCTION

The measurement of fluid flow is critical in several industries including oil and gas, public utilities, food and beverage, and turbine engine testing. While the required degree of accuracy for flow measurement varies for each of these industries, the need for accurate measurement boils down to the same reason: the almighty dollar. In turbine engine applications, specific fuel consumption (SFC) is a key parameter for determining the flight cost of a jet engine. Specific fuel consumption is the fuel flow rate divided by thrust. Similar to the way that miles-per-gallon is used for ground vehicles, specific fuel consumption is used as the overall indicator of fuel efficiency for an aircraft engine. It is used to determine an aircraft's range, payload, and optimum cruising speed. Figure 1 [11] shows a plot of SFC vs. thrust, referred to as a power hook, for a generic turbine engine application. The minimum value of SFC along the power hook is used as the flight setting for cruise power. Accurate measurement of fuel flow is necessary to determine the capabilities of any aircraft engine application.

The qualification process for turbine engines typically involves a ground test in a test facility that is capable of simulating the pressures and temperatures of the flight conditions at which the engine is expected to operate. Qualification criteria are generally provided to the engine manufacturer by the aircraft manufacturer. A qualification test will involve taking steady state data points at various throttle settings while holding the simulated flight condition constant. The steady state data will then be compared to the qualification criteria to determine

whether or not the engine can be fully qualified for the application. With increasing fuel costs and a strong field of competitors, the qualification criteria for aircraft engines are more stringent than ever before. Modern aircraft engines, especially military engines, are often on the very edge of the pass/fail criteria for SFC. Because the margin between the SFC of a test article (engine) and the qualification criteria is often so small, a qualification test must have the smallest uncertainty possible on fuel flow and thrust.

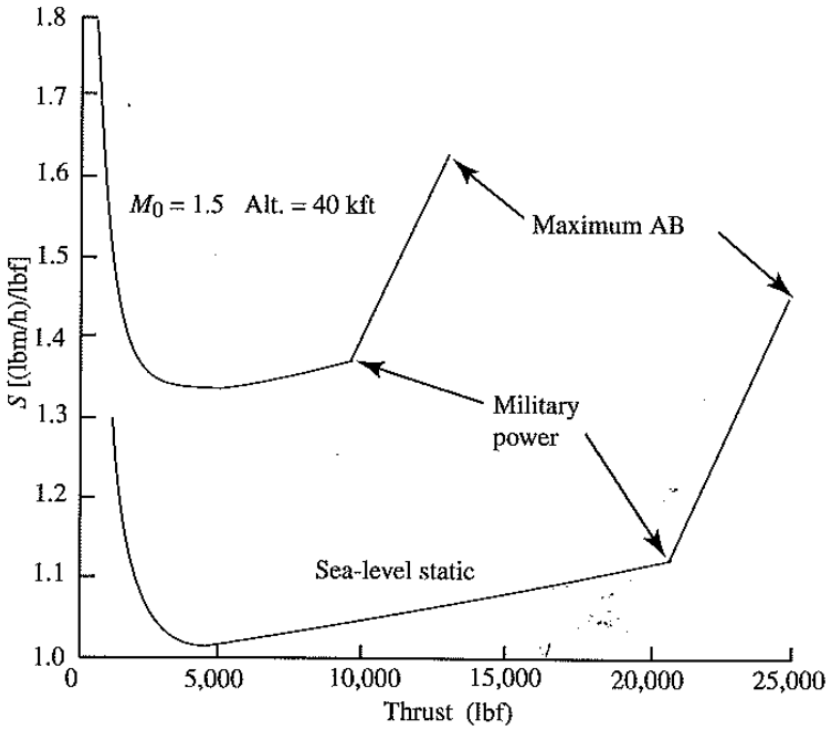

Figure 1. Example of a Power Hook for a Turbine Engine [11]

Arnold Engineering Development Complex is the Air Force's premier ground test complex for aerospace testing, particularly for turbine engine testing.

The uncertainty of thrust measurement in the turbine engine test cells at AEDC has been developed continuously over the years, and well thought out processes are in place for estimating thrust uncertainty. However, the process of developing fuel flow uncertainty estimates became almost a lost art at AEDC through the early 2000's. Advancements in instrumentation and calibration practices were not always considered or fully understood when quoting fuel flow uncertainty for current projects. In many cases, "canned" values for fuel flow uncertainty that had been developed several years prior to a project were quoted as current uncertainty estimates. This practice led AEDC to develop new uncertainty procedures for estimating fuel flow uncertainty. This thesis endeavors to determine the fuel flow uncertainty for an altitude test facility at Arnold Engineering Development Complex, located at Arnold Air Force Base, TN. A suggested method will be presented for determining the uncertainty of fuel flow for the test facility.

2.0 MEASUREMENT UNCERTAINTY CONCEPTS

The term “measurement uncertainty” is a concept that helps to describe the overall goodness of a quantity being measured. Because no measurement has or can ever be taken with 100% accuracy, it becomes necessary to provide some level of assurance to say how close the measurement is to the true value. The terminology and methodology used for the uncertainty analysis presented herein is compliant to the ASME standard for measurement uncertainty, PTC19.1-2005 [4]. The uncertainty model presented in Ref. 4 categorizes elemental error sources (and their respective uncertainties) as either systematic or random, which is determined by the effect that the error source has on the measured data. These concepts will be discussed in more detail in this section. Another uncertainty model, the Guide to the Expression of Uncertainty in Measurement [7] (referred to as the GUM), does not categorize elemental error sources but does categorize uncertainties as either Type A or Type B depending on the method used to determine the level of uncertainty for the error source. The GUM method will be described briefly in section 2.8.

2.1 MEASUREMENT ERROR

In a perfect measurement system, the value that is determined by a measurement system would be the exact value of the object being measured. However, all measurement systems are inherently flawed to some degree. Therefore, every measurement has some amount of associated error. Simply

stated, measurement error is the amount by which the measured quantity deviates from the true value of the object undergoing measurement. Measurement error consists of two components: random error and systematic error. These components will be discussed in detail in the following sections. Figure 2 shows these components for a single measurement taken out of a normally distributed population of measurements. Improving the accuracy of a measurement system involves reducing both the random and systematic error of the system, as shown in Figure 3.

2.1.1 Random Error

Random error is the portion of the total error that varies randomly about the true value with repeated measurements. Any source of error that adds scatter to a data set is said to cause random error [2]. Random error may arise from nonrepeatabilities of a measurement system, variations in environmental conditions, variations in measurement technique, etc. The total random error for a measurement is usually the combination of several random error sources.

2.1.2 Systematic Error

Systematic error is the portion of the total error that remains constant with repeated measurements. The systematic error cannot be determined unless the measurement is compared to the true value of the quantity measured. Since the true value is itself unknown, calibrations should be performed to reduce the amount of systematic error in a measurement system. Although a calibration

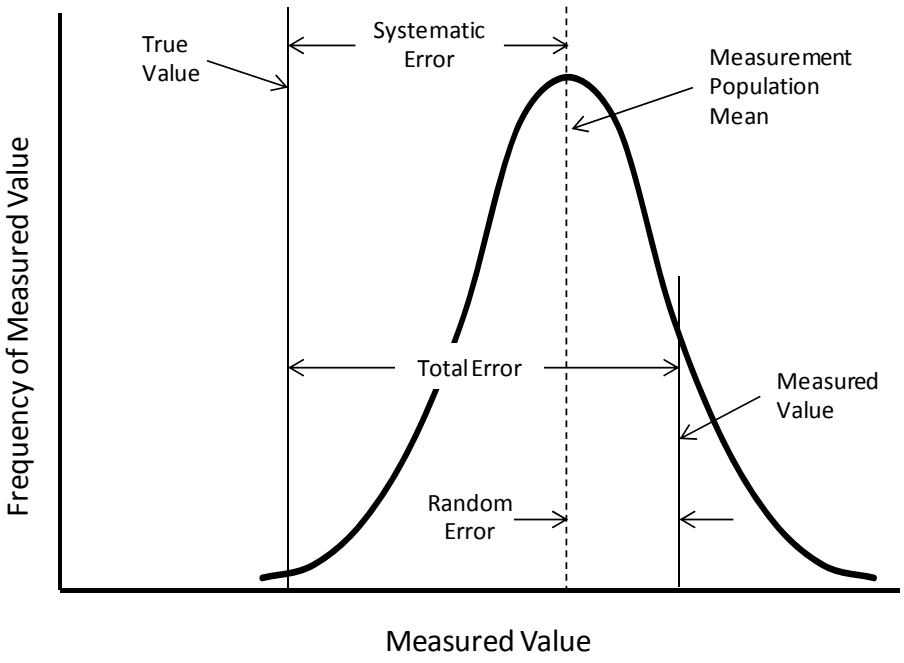

Figure 2. Measurement Error

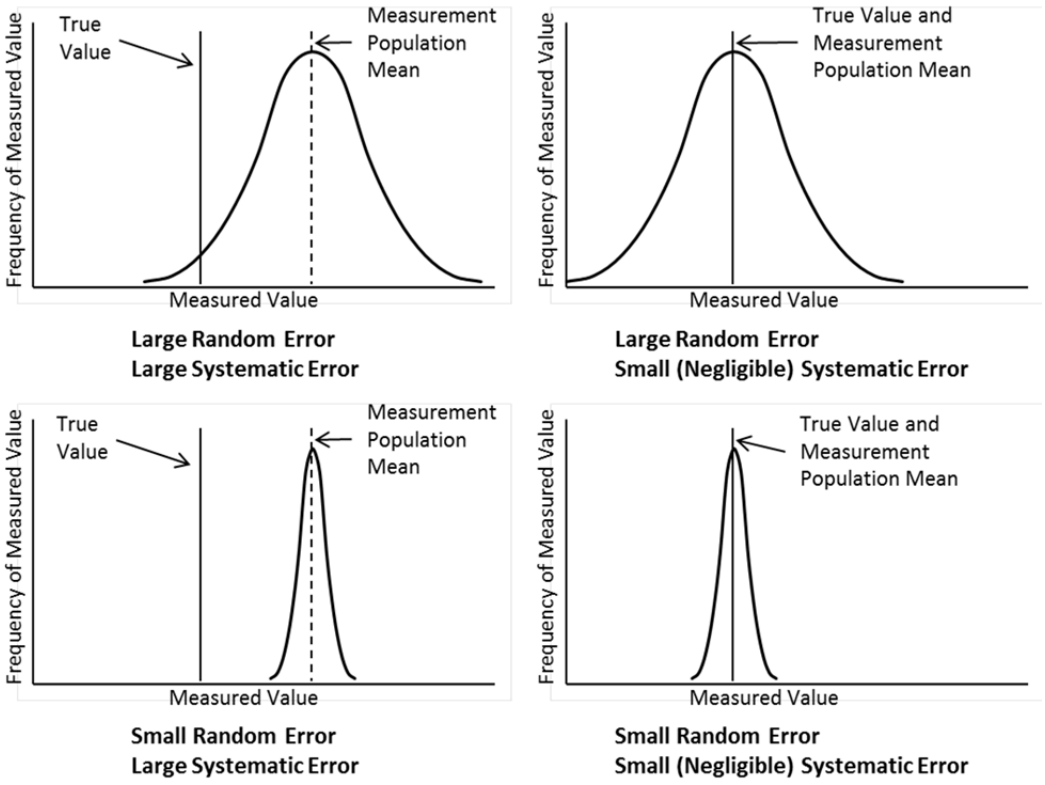

Figure 3. Random and Systematic Error

itself will impart some error into the system, it can be used to greatly reduce large known systematic errors. Common sources of systematic error include calibrations, instrumentation manufacturing deficiencies, unknowns in the measurement system, data reduction technique, etc. The total systematic error for a measurement is usually the combination of several systematic error sources. Systematic error can be categorized as known or unknown.

2.1.2.1 Known Systematic Errors

If the magnitude of a systematic error for an instrument is known, by comparison to a standard instrument or by measuring a standard quantity for example, the error may be corrected by applying a correction factor or a calibration to the instrument.

2.1.2.2 Unknown Systematic Errors

If the magnitude of a systematic error for an instrument is unknown, it cannot be corrected by applying a correction factor or a calibration. Every effort should be made to identify and eliminate all elemental sources of systematic error in a measurement system. A thorough knowledge of the measurement system is required to do this. Although it is not possible to completely eliminate all of the systematic error from a system, human errors (such as improper calibrations or installations) and unexpected environmental disturbances/conditions (such as shocks or bad flow profiles) can be identified by following quality control processes. Calibration histories and comparisons to

historical data can provide an idea of the drifts, trends, and movements of a measurement system.

2.2 MEASUREMENT UNCERTAINTY

The measurement error of a system can never be perfectly quantified or fully known. This necessitates the use of a parameter called measurement uncertainty that is an estimate of the measurement error. The measurement uncertainty can be thought of as a boundary around a measured value within which the true value is *reasonably* expected to reside *most of the time*. The key terms "reasonably" and "most of the time" are important to understand in the context of measurement uncertainty. Uncertainty should always be expressed as a confidence interval that is expected to contain the true value with a given level of confidence. For example, if a parameter has a true value of 10.0, and the measurement uncertainty at the 95% confidence level is equal to 1.0, then approximately 95 out of every 100 random, independently-measured samples should reside within the interval of 9.0 – 11.0 (Figure 4). The term "reasonably" is used in the definition of measurement uncertainty due to the indefinable nature of measurement error and because uncertainty is not an exact determination of error; it is an estimate. "Most of the time" is used in the description of measurement uncertainty to capture the idea that uncertainty in a given measurement is not expected to include the true value with 100% accuracy but that it is only an estimate with a given level of confidence. The random and systematic components of measurement error can be estimated by the random

and systematic uncertainties of a measurement. These components can then be combined to estimate the total error in a system. This section will describe the basic method used to estimate the uncertainty in a system.

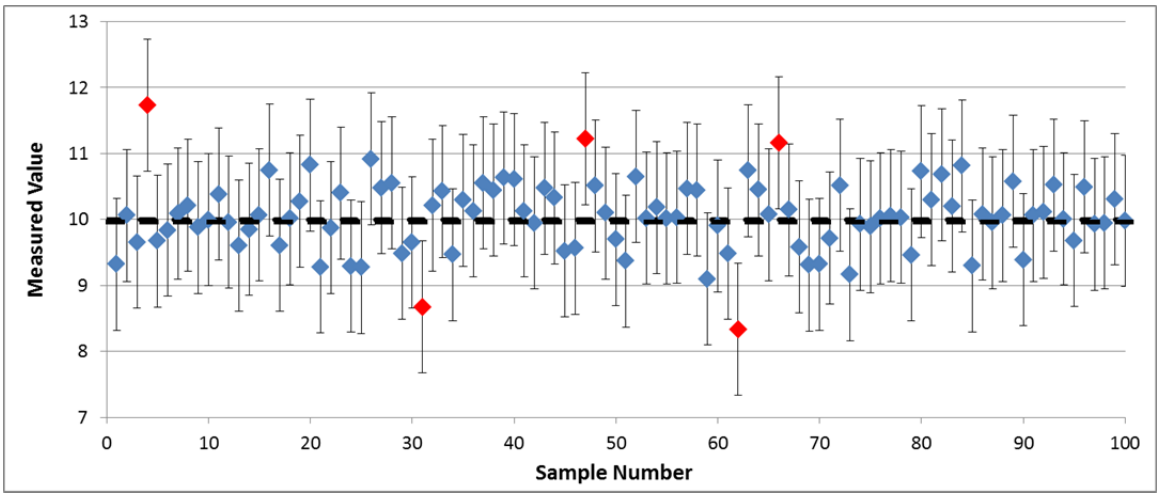

Figure 4. Random Sampling of a True Value of 10 with 95% Confidence Uncertainty Bars

2.2.1 Random Uncertainty

For any given measurement, there exist several sources of random error. These error sources will add scatter to the measurement data. The random uncertainty of a measurement is an estimate of the overall random error. It can be calculated by taking the standard deviation of a dataset of size N, as follows:

$$s_X = \sqrt{\sum_{i=1}^{N} \frac{(X_i - \overline{X})^2}{N - 1}} \qquad (1)$$

where $\overline{X}$ is the average of the data set:

$$\overline{X} = \sum_{i=1}^{N} \frac{X_i}{N} \quad \textbf{(2)}$$

The random uncertainty can also be estimated by using the difference between identical instruments taking readings of the same object at the same time. Assuming that identical instruments are used to measure the same parameter at the same moments in time, the standard deviation of the deltas between the two instruments is representative of the standard deviation of the individual devices, as follows:

$$s_X = \sqrt{\sum_{i=1}^{N} \frac{(\Delta_i - \bar{\Delta})^2}{2(N-1)}} \quad \textbf{(3)}$$

This method will hold true even if the measured parameter varies in magnitude or if the two instruments have differing systematic errors. An example of this might be two thermometers, in close vicinity in a controlled environment, reading air temperature. This provides an excellent method of estimating the random uncertainty of a device (or devices) when the parameter being measured is constantly in flux.

The number of degrees of freedom associated with a standard deviation is an important part of a measurement uncertainty analysis. Degrees of freedom

will be discussed more in Section 4.4. Suffice it to say here that the number of degrees of freedom (ν) associated with a standard deviation is equal to N-1.

2.2.2 Systematic Uncertainty

For any given measurement, there are several sources of systematic error. These errors will remain constant from measurement to measurement. The systematic uncertainty of an error source is an estimate of the systematic error. Once an elemental systematic error source has been identified, the uncertainty due to that error is typically estimated using one of three methods:

- Published information
- Special data
- Engineering judgment

2.2.2.1 Published Information

Information on the systematic uncertainty of an error source is often available in publication from calibration reports, manufacturer's specifications, previous tests, or other technical references. When using published uncertainties, care must be taken to ensure that the proper confidence interval is assumed for the uncertainty. Manufacturer's specifications may be quoted at the 95% or 99% confidence interval, but this information is often missing or misleading in the manufacturer's documentation. Caution is necessary when applying manufacturer's specifications to an uncertainty analysis. Unless other information is available, the number of degrees of freedom for published systematic uncertainties is assumed to be infinity.

2.2.2.2 Special Data

In some cases special data may be obtained that can be used to estimate the systematic standard deviation of a measurement instrument or system. Two of these methods are:

1. Interlaboratory or interfacility tests (such as a round-robin flowmeter calibration) and
2. Comparison of independent measurements that are made on systems that depend on different principles or on independently calibrated systems.

The systematic uncertainty for the measurement can then be calculated by taking the standard deviation of the independently obtained special data and dividing by the square root of the number of independent special samples obtained.

2.2.2.3 Engineering Judgment

If no published information or special data is available, engineering judgment can be used to estimate the value of the systematic uncertainty of an error source. This requires a thorough knowledge of the test apparatus, test process, and test objectives. Uncertainty estimates made from engineering judgment are assumed to be made at the 95% confidence level (two standard deviation level). The number of degrees of freedom for these uncertainties is assumed to be infinity [2]. To obtain the systematic uncertainty at the one standard deviation level, the systematic uncertainty obtained through engineering judgment should be divided by two [2].

2.3 COMBINED UNCERTAINTY

The total uncertainty for a measurement is the combination of the random and systematic uncertainty in the measurement. Once the random and systematic uncertainties at the one standard deviation level have been determined, the combined uncertainty at the one standard deviation level can be found using the following:

$$u_X = \sqrt{(s_X)^2 + (b_X)^2} \quad \textbf{(4)}$$

Note that u_X is expressed at the single standard deviation level, which is the 68% confidence interval. Confidence intervals will be discussed further in Section 2.6.

2.4 PROPAGATION OF UNCERTAINTY TO A RESULT

Complex measurement systems are made up of many components and often involve complex calculations. Every component or measurement made within the system (i.e. pressure and temperature measurement) or assumption made about the system (i.e. calibration coefficient) contributes uncertainty toward the final result (i.e. flow rate through a meter). Uncertainty propagation is the method by which the uncertainties in individual measurements are combined to determine the uncertainty of a result. Naturally, some parameters will have a greater influence on the result than others. The influence coefficient for each input parameter must be determined to propagate uncertainties to the result.

Three methods are generally used for uncertainty propagation: Taylor's Series method (TSM) using closed form solutions, dithering (also known as the perturbation method, a numerical approach to the TSM), and Monte Carlo method (MCM). The uncertainty analysis reported in Section 4 was conducted using dithering and MCM. All three methods are described briefly in this section.

2.4.1 Taylor's Series Method

The Taylor's Series uncertainty propagation is defined in great statistical detail in Refs. 1 and 12. The derivation will be shown here for a function of two variables before a more general case is given. The function of interest is:

$$r = r(x, y) \tag{5}$$

where x and y each have systematic and random errors, β_{xi} and ϵ_{xi}, respectively, for the ith set of measurements (x_i, y_i).

Applying a Taylor's series expansion to the function r yields:

$$r_i = r_{true} + \theta_x(x_i - x_{true}) + \theta_y(y_i - y_{true}) + \text{higher order terms} \tag{6}$$

where

$$\theta_x = \frac{\partial r}{\partial x} \quad and \quad \theta_y = \frac{\partial r}{\partial y} \tag{7}$$

The θ terms here are referred to as influence coefficients. The higher order terms are generally assumed to be negligible compared to the first order terms. This is a reasonable assumption when the first order terms have large influence coefficients and the total errors, $x_i - x_{true}$, in x and y are reasonably small. When these two criteria are met, the higher order terms (which raise the errors to the 2nd, 3rd, etc. powers) will tend to approach zero much faster than the first order terms. For the special case where r is a linear function, the higher order partial derivatives will be exactly 0.

Neglecting the higher order terms, the total error in r can then be defined as:

$$\begin{aligned} \delta_{r_i} = r_i - r_{true} &= \theta_x \delta_{x_i} + \theta_y \delta_{y_i} \\ &= \theta_x(\beta_{xi} + \epsilon_{xi}) + \theta_y(\beta_{yi} + \epsilon_{yi}) \end{aligned} \tag{8}$$

The variance of the population of potential values of r is defined as:

$$\sigma_r{}^2 = \lim_{N\to\infty}\left(\frac{1}{N}\sum_{i=1}^{N}\left(\delta_{r_i}\right)^2\right) \tag{9}$$

Substituting the total error equation into the variation equation (the limits from n to infinity are omitted) yields:

$$\begin{aligned}
&\frac{1}{N}\sum_{i=1}^{N}\left(\delta_{r_i}\right)^2 \\
&\quad = \theta_x{}^2\frac{1}{N}\sum_{i=1}^{N}\left(\beta_{x_i}\right)^2 + \theta_y{}^2\frac{1}{N}\sum_{i=1}^{N}\left(\beta_{y_i}\right)^2 \\
&\quad + \theta_x{}^2\frac{1}{N}\sum_{i=1}^{N}\left(\epsilon_{x_i}\right)^2 + \theta_y{}^2\frac{1}{N}\sum_{i=1}^{N}\left(\epsilon_{y_i}\right)^2 \\
&\quad + 2\theta_x\theta_y\frac{1}{N}\sum_{i=1}^{N}\beta_{x_i}\beta_{y_i} + 2\theta_x\theta_y\frac{1}{N}\sum_{i=1}^{N}\epsilon_{x_i}\epsilon_{y_i} \\
&\quad + 2\theta_x{}^2\frac{1}{N}\sum_{i=1}^{N}\beta_{x_i}\epsilon_{x_i} + 2\theta_y{}^2\frac{1}{N}\sum_{i=1}^{N}\beta_{y_i}\epsilon_{y_i} \\
&\quad + 2\theta_x\theta_y\frac{1}{N}\sum_{i=1}^{N}\beta_{x_i}\epsilon_{y_i} + 2\theta_x\theta_y\frac{1}{N}\sum_{i=1}^{N}\epsilon_{x_i}\beta_{y_i}
\end{aligned} \tag{10}$$

Substituting in the variances for β and ϵ on the variables x and y and assuming that no systematic/random correlations exist ($\beta\epsilon$ terms are zero) results in the following:

$$\sigma_r{}^2 = \left(\theta_x \sigma_{\beta_x}\right)^2 + \left(\theta_y \sigma_{\beta_y}\right)^2 + \left(\theta_x \sigma_{\epsilon_x}\right)^2 + \left(\theta_y \sigma_{\epsilon_y}\right)^2 + 2\theta_x \theta_y \sigma_{\beta_x \beta_y} + 2\theta_x \theta_y \sigma_{\epsilon_x \epsilon_y} \quad \textbf{(11)}$$

The actual variances of the systematic and random errors are never actually known, which leads back to the use of uncertainty for an estimate of the errors in the measurement. The uncertainty in r is then given as:

$$u_r{}^2 = (\theta_x b_x)^2 + \left(\theta_y b_y\right)^2 + (\theta_x s_x)^2 + \left(\theta_y s_y\right)^2 + 2\theta_x \theta_y b_{xy} + 2\theta_x \theta_y s_{xy} \quad \textbf{(12)}$$

The terms b_{xy} and s_{xy} are estimates of the covariance for the systematic and random errors, respectively. If the variables x and y are completely independent, then the covariance can be assumed to be zero. However, if a correlation exists between the measurements of x and y, then the covariance should be included in the uncertainty propagation equation. Assuming that all of the error sources are independent, the general equation for the uncertainty of the result can be given as:

$$u_r = \sqrt{\sum_{i=1}^{N} (\theta_i b_i)^2 + \sum_{i=1}^{N} (\theta_i s_i)^2} \qquad \textbf{(13)}$$

2.4.2 Dithering Method

The dithering method for uncertainty propagation uses the same uncertainty propagation equation that was just derived for the Taylor's Series method. However, rather than calculating the influence coefficients analytically, the dithering method utilizes modern computing power and the data reduction program to compute the influence coefficients numerically. The steps for determining the influence coefficients through dithering are as follows:

1) The data reduction program is used to calculate the experimental result. The result calculated initially is referred to as r_{init} .
2) Each input parameter on which the experimental result is dependent is increased (or decreased) by a small, convenient amount, commonly 0.1% (Eq. 14), 1°F, 1 psia, etc. This factor will be referred to from hereon as the perturbation factor. The new values for the input parameters are referred to as the perturbated values (x_{pert}).

$$x_{pert} = x_{init} * 1.001 \qquad \textbf{(14)}$$

3) The result is recalculated using the perturbated value for one input parameter and the original values for the remaining input parameters (Eq. 15). This step is repeated for each of the input parameters.

$$r_{pert} = f(x_{pert}, \text{other initial variables}) \quad \textbf{(15)}$$

4) The influence coefficient for an input parameter is then equal to the difference between the initial and perturbated values of the result divided by the difference between the initial and perturbated input values (Eq. 16). The influence coefficient can also be converted to a relative influence coefficient, as shown in Eq. 17. The relative influence coefficient will be used in the analysis in Section 4 and is often more useful in practice than the absolute influence coefficient.

$$\theta_X = \frac{\Delta r}{\Delta x} = \frac{r_{pert} - r_{init}}{x_{pert} - x_{init}} \quad \textbf{(16)}$$

$$\theta_X{}' = \theta_X * \frac{x_{init}}{r_{init}} = \frac{\Delta r}{\Delta x} * \frac{x_{init}}{r_{init}} \quad \textbf{(17)}$$

The method just described assumes that the uncertainty of the experimental result is symmetrical about each of the input parameters. This is almost always a safe assumption to make. However, if an inflection point exists near the value of the result, the influence coefficient may change depending on

whether a positive or negative perturbation factor is used. If this is expected to be an issue, the influence can be calculated using positive and negative perturbation factors and compared to ensure that the distribution is symmetrical about the point of interest.

Once all of the influence coefficients have been calculated, the combined uncertainty is found by root-sum-squaring the products of the influence coefficients with the individual systematic and random uncertainties for each input parameter.

2.4.3 Monte Carlo Method

The Monte Carlo method of uncertainty propagation is a powerful method that is most useful for extremely complex equations and/or for systems with correlated errors. Like the dithering method, Monte Carlo utilizes the computer software that is used to calculate the result. The steps for a Monte Carlo uncertainty simulation are as follows:

1) Assign an error distribution and one-standard deviation uncertainty interval to each of the input parameter error sources. Systematic and random error sources are treated similarly in this method.
2) Use a random number generator to select values for each error source within the assigned error distributions and uncertainty intervals.
3) Add the error values back to their respective input parameter values, and calculate the experimental result using the new values for the input parameters.

4) Repeat steps 2 and 3 several times. Hundreds or thousands of repetitions are not uncommon for this type of analysis.

5) Calculate the standard deviation of the results that were calculated in step 4. The standard deviation of the results is then the uncertainty of the result at the one standard deviation level. (This assumes that the distribution is symmetric about the average value.) The convergence of the standard deviation can be used as the stop criteria for step 4.

6) Multiply the standard deviation by 2 to obtain the 95% confidence interval.

The Monte Carlo method requires the most computing power and time of the three methods used, but it does yield a correct uncertainty interval and can be simpler than the Taylor's Series method when dealing with correlated uncertainties and very complex equations.

It should be noted the Monte Carlo method can result in non-symmetric distributions if the uncertainty of a particular variable is relatively large or if the equations used to calculate the result are highly non-linear. In these cases, special methods should be employed to determine the true 95% coverage interval. A method of determining the confidence is given in Ref. 1.

2.5 DEGREES OF FREEDOM AND CONFIDENCE INTERVALS

The number of degrees of freedom is used in association with the Student's t-table to determine the multiplier to be used on u_X to achieve the desired coverage interval. By integration (area under the curve), one standard

deviation (1σ) provides the 68% coverage interval. This means that an independent and randomly measured data point has a 68% chance of falling within one standard deviation of the population average. Stated alternatively, 68% of the independent and randomly selected data should fall within one standard deviation of the population average. The 95% coverage interval is desired when quoting the uncertainty for most applications. To expand the coverage interval from 68% to 95%, u_X is multiplied by the Student's t-value (referred to as t_{95}) taken from the Student's t-table for the number of DOF associated with the uncertainty estimate. For example, to achieve the 95% coverage interval with 30 DOF, a multiplier of 2.042 is applied to the standard deviation. For an uncertainty estimate with only 10 DOF, the value of t_{95} increases to 2.228. Note that both the ASME method [4] and the ISO method [7] advocate the use of 2 for t_{95} when the number of DOF is 30 or more. For some applications, uncertainty may be quoted at the 3σ level, which is the 99.5% confidence interval (assuming large number of DOF). The 1σ, 2σ, and 3σ confidence intervals are shown in Figure 5.

2.5.1 Welch-Satterthwaite Formula

The Welch-Satterthwaite formula [1, 2, 4] can be used to calculate the number of degrees of freedom of the result, ν_r, as follows:

$$\nu_r = \frac{\left[\sum_{i=1}^{K}(s_i)^2 + \sum_{i=1}^{K}(b_i)^2\right]^2}{\sum_{i=1}^{K}\frac{(s_i)^4}{\nu_{s_i}} + \sum_{i=1}^{K}\frac{(b_i)^4}{\nu_{b_i}}} \quad \textbf{(18)}$$

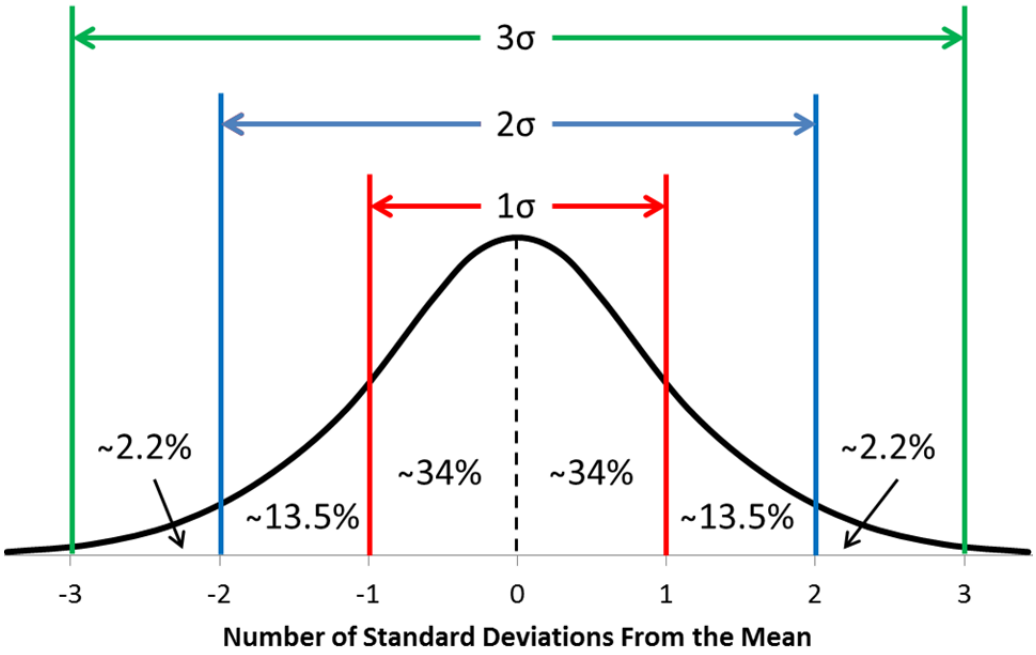

Figure 5. Confidence Intervals Expressed as Standard Deviations

where ν_{s_i} and ν_{b_i} are the degrees of freedom of the i^{th} elemental random and systematic uncertainties, respectively.

The value of ν_r is then used to determine the appropriate t-value to use for the desired coverage interval. The uncertainty of the result with a 95% coverage interval is then given by the following:

$$U_{95} = t_{95} u_r = t_{95} \sqrt{\sum_{i=1}^{N} (\theta_i b_i)^2 + \sum_{i=1}^{N} (\theta_i s_i)^2} \qquad (19)$$

Commonly, expanded uncertainty is denoted with an upper-case U, with the subscript indicating the coverage interval for the expanded uncertainty (i.e. 95%, 99%, etc.).

2.5.2 Large Sample Assumption

The large sample assumption is commonly used in engineering practice to eliminate the problem of keeping up with the number of degrees of freedom for each individual source of uncertainty in a complex calculation. Since complex calculations involve many variables with varying numbers of degrees of freedom, and since most systematic uncertainties are estimated with a large number of degrees of freedom (commonly, $\nu_{b_k} = \infty$), the total number of degrees of freedom for the result, ν_r, can safely be assumed to be greater than 30 in nearly all engineering applications where sufficient data has been collected to perform an uncertainty analysis. The t-value for the 95% coverage interval for the uncertainty of the result is simply assumed to be 2. This assumption greatly reduces the complexity of the uncertainty analysis, as the degrees of freedom for each individual elemental uncertainty component need not be retained. The large sample assumption holds true unless one uncertainty component dominates the uncertainty in the result and has a very low number of degrees of freedom. Since the Welch-Satterthwaite equation uses the random and systematic uncertainties raised to the 4^{th} power in the denominator, if one uncertainty component dominates the uncertainty with a small number of

degrees of freedom, this will tend to drive down the number of degrees of freedom of the result. For this reason, it is always good practice for the person running an experiment to remain cognizant of the amount of data he has acquired in order to ensure that the large sample assumption will hold true. For this analysis, the large sample assumption will not be applied, so that the Welch-Satterthwaite formula will be utilized to find the number of degrees of freedom of the result.

2.6 ALTERNATIVE UNCERTAINTY MODELS

While the definitions of random and systematic (formerly known as precision and bias, respectively [3]) uncertainty and the methods used to determine the levels of uncertainty have changed little over the years, several models have been used in the past to combine the random and systematic components of uncertainty. The uncertainty model described up to this point and used throughout this paper is the ASME model, also referred to as the U_{95} model, as described in Ref. 1, 2, and 4. Much of the older literature on measurement uncertainty utilizes two methods that differ from the U_{95} method: the addition (U_{ADD}) model and the root-sum-square (U_{RSS}) model. Another model, referred herein as U_{ISO}, uses a different classification system for uncertainty components. These alternative uncertainty models are explained here for reference.

2.6.1 Historical Uncertainty Models

The U_{ADD} and U_{RSS} uncertainty models are presented in detail in Ref. 3. The U_{ADD} model uses the following equation for the combined uncertainty:

$$U_{ADD} = B_R + t_{95} S_R \quad \textbf{(20)}$$

where B_R is the systematic uncertainty of the result, equal to $2 * b_R$, and S_R is the root-sum-square of the elemental random uncertainties at the single standard deviation level. In the U_{ADD} uncertainty model, the elemental systematic uncertainties (B_i) can be combined by either root-sum-squaring them for a close approximation to the actual error or by adding them to achieve a conservative estimate of the error. The method used to combine the B_i's is left to the discretion of the analyst. U_{ADD} covers approximately the 99% confidence interval [3].

The U_{RSS} model uses the following equation for the combined uncertainty:

$$U_{RSS} = \sqrt{B_R + t_{95} S_R} \quad \textbf{(21)}$$

where B_R and S_R are equivalent to the U_{ADD} method. The U_{RSS} uncertainty model covers approximately the 95% confidence interval [3].

Neither the U_{ADD} nor the U_{RSS} models should be used in common practice today. For all intents and purposes, the industry has adopted newer, improved models, the U_{95} model and the U_{ISO} model.

2.6.2 ISO Uncertainty Model

The ISO uncertainty model is presented in detail in the "Evaluation of Measurement Data — Guide to the Expression of Uncertainty in Measurement" [7] published by the Joint Committee for Guides in Metrology (JCGM). The JCGM is a conglomerate organization with the following member organizations: the International Bureau of Weights and Measures (BIPM), the International Electrotechnical Commission (IEC), the International Federation of Clinical Chemistry and Laboratory Medicine (IFCC), the International Organization for Standardization (ISO), the International Union of Pure and Applied Chemistry (IUPAC), the International Union of Pure and Applied Physics (IUPAP), the International Organization of Legal Metrology (OIML), and the International Laboratory Accreditation Cooperation (ILAC). Originally published as the "Guide to the Expression of Uncertainty in Measurement" by ISO, it is still colloquially referred to as the "ISO GUM". A useful addition to the ISO GUM is the "International Vocabulary of Metrology" [9], which provides thorough definitions and explanations of the terminology used throughout the ISO GUM.

The ISO GUM uncertainty model is built around the concept of classifying uncertainties based on the method used to derive or evaluate them. If the elemental uncertainty was derived using a statistical approach on current test

data, then it is categorized as a Type A uncertainty. All uncertainties that were not derived using a statistical approach using current test data are characterized as Type B. Type B uncertainties are typically based on engineering judgment using any of the following relevant information on the measurement system [10]:

- previous measurement data,
- experience with, or general knowledge of, the behavior and property of relevant materials and instruments,
- manufacturer's specifications,
- data provided in calibration and other reports, and
- uncertainties assigned to reference data taken from handbooks.

While there is no direct correlation between the uncertainty characterization used in the ASME model (random and systematic) and the characterization used in the ISO model (Type A and Type B), the random uncertainties from ASME model often fit into the Type A characterization, and systematic uncertainties often fit into the Type B characterization. However, this is not always the case, and it is important for the analyst to understand that the terminology of the ASME and ISO uncertainty models cannot be used interchangeably.

The ISO uncertainty model uses the following equation for the combined uncertainty:

$$U_{ISO} = k\sqrt{(U_A)^2 + (U_B)^2} \quad \textbf{(22)}$$

where k is the value of Student's t for the degrees of freedom calculated with the Welch-Satterthwaite formula. It is noteworthy that U_{ISO} will yield the same result as U_{95}. Therefore, the major difference between the ISO and the ASME approach remains the categorization of elemental uncertainties, which should not affect the final uncertainty result.

3.0 METHOD OF FUEL FLOW MEASUREMENT

3.1 VOLUMETRIC TURBINE FLOWMETERS

3.1.1 Anatomy of a Turbine Flowmeter

The devices used to measure fuel flow in this application are volumetric turbine flowmeters. A cutaway picture of a typical volumetric turbine flowmeter is shown in Figure 6 [13].

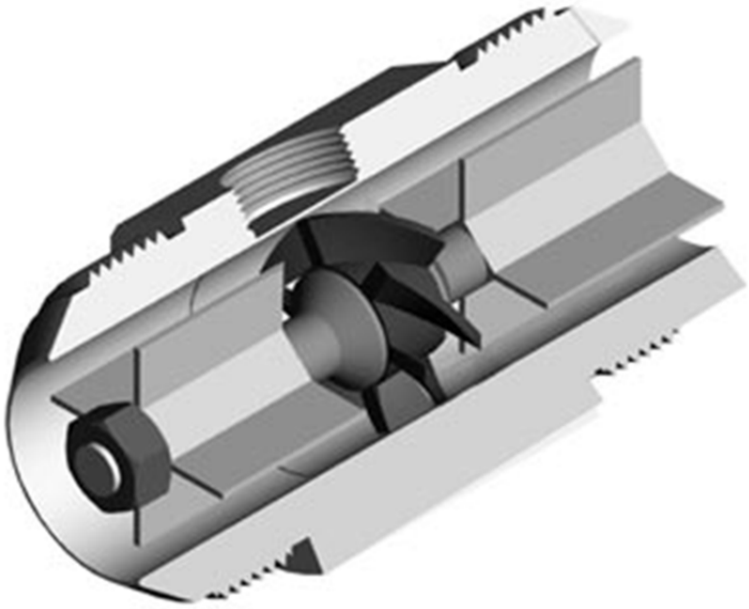

Figure 6. Cutaway of a Single Rotor Turbine Flowmeter [13]

Figure 7 [13] is a conceptual diagram showing the important features of a turbine flowmeter. The flow going through the meter spins the rotor in the middle of the meter. As its name implies, a volumetric turbine flowmeter does not

directly measure mass flow rate but rather volumetric flow rate. The rotational velocity of the rotor is correlated to a certain volumetric rate of fluid flow through the meter. The electronic pickup shown in Figure 7 is the only direct measurement taken off of the meter itself.

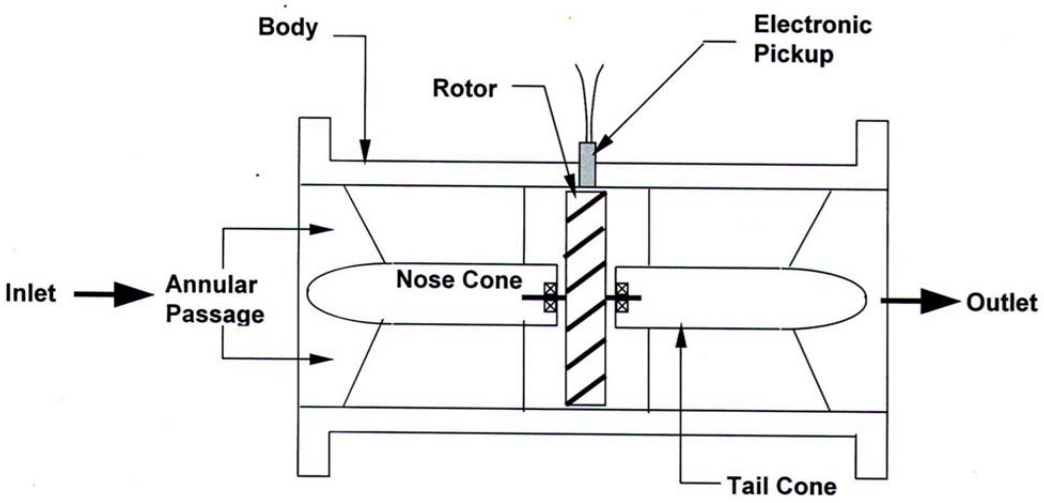

Figure 7. Turbine Flowmeter Concept Diagram [13]

3.1.2 Calibration Method

The flowmeters for this application are calibrated using a positive displacement flow calibration bench. The calibration bench utilizes a positive displacement pump to drive a piston through a cylinder of known cross-sectional area. Measurements of the distance and time of travel of the piston through the cylinder are used to calculate the volumetric flow rate through the device. The frequency output of the flowmeter is then used to develop a calibration coefficient for the meter. The flowmeters are calibrated at many flow rates throughout the

measureable range of the meter. The calibration fluid is a mixture of propylene glycol and water that closely matches the kinematic viscosity of the fuel that is measured in the test environment. A flowmeter calibration bench (located at University of Tennessee Space Institute in Tullahoma, TN) is shown in Figure 8.

Figure 8. Flowmeter Calibration Setup

The flowmeter response to various flow rates can be characterized by the relationship of volume flow rate (or flow rate divided by frequency) to meter frequency, but such a calibration would only be applicable for the exact viscosity, temperature, and pressure of the fluid during the calibration. An improved characteristic is the universal viscosity curve, which gives the meter K-factor (frequency/volume flow rate) as a function of the frequency over viscosity, as shown in Figure 9 [13]. The K-factor gives an indication of how much of the working fluid will pass through the meter for a given pulse.

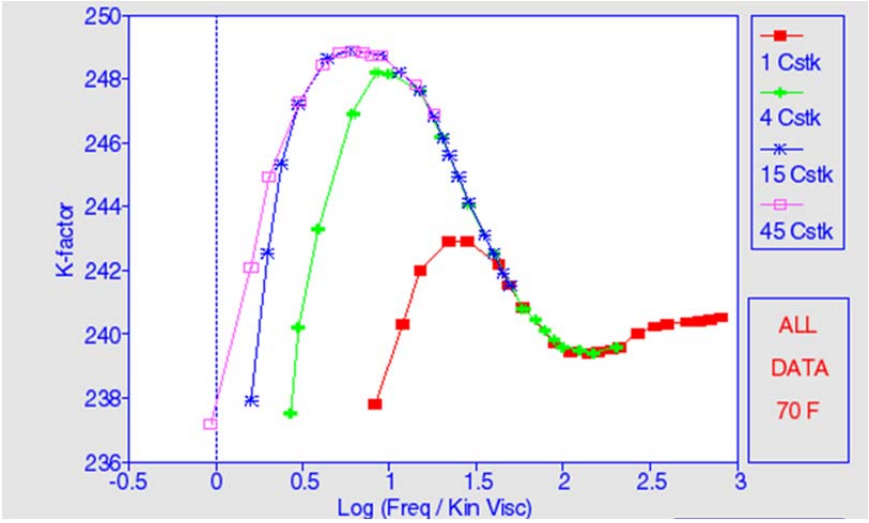

Figure 9. Universal Viscosity Curve at Constant Temperature [13]

Although the universal viscosity curve removes variations due to viscosity, it is still susceptible to variations in temperature and (to a lesser degree) pressure, as shown in Figure 10 [13]. The non-dimensional parameters, Strouhal number and Roshko number, provide a relationship that can be used over a variety of temperatures and pressures. Fundamentally, the Strouhal number and Roshko number are the K-factor and frequency over viscosity parameter, respectively, that have been corrected to a specific temperature and pressure. These two dimensionless parameters are calculated using the following:

Strouhal number: $$St = \frac{f\,D}{U} = \frac{\pi\,K\,D^3}{4}$$

Roshko number: $$Ro = \frac{f\,D^2}{\nu}$$

where: $$D = D_0[1 + \alpha(T - T_0)]\left[1 + \frac{D_0(p - p_0)}{2tE}\right]$$

D_0 = Reference Diameter
T_0 = Reference Temperature
p_0 = Reference Pressure
α = Coefficient of Fuel Thermal Expansion
E = Flowmeter Modulus of Elasticity
T = Measured Fuel Temperature
p = Measured Fuel Pressure
t = Flowmeter Wall Thickness
U = Flow Velocity
f = Flowmeter Frequency
K = K − factor, Pulses per Volume
ν = Kinematic Viscosity

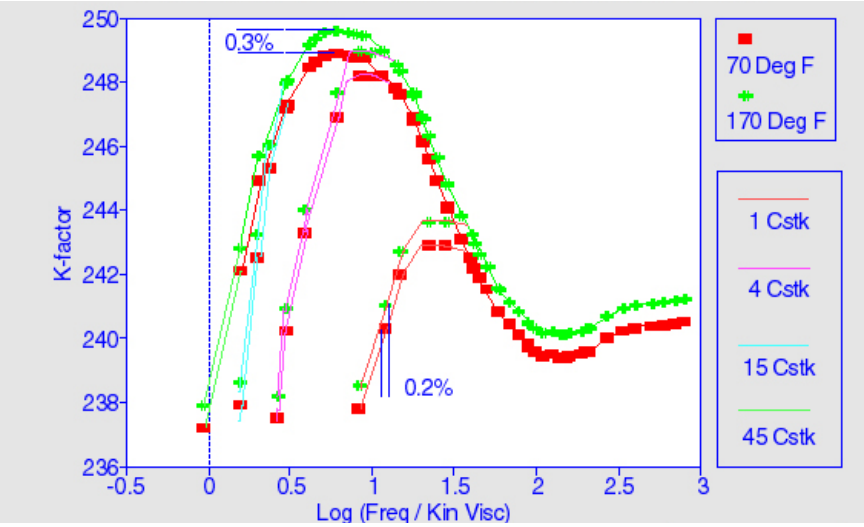

Figure 10. Universal Viscosity Curve with Varying Temperature [13]

The calibration curve using Strouhal number and Roshko number can then be used to calculate the flow rate of a working fluid with any viscosity, temperature, and pressure within the valid calibration region for the flowmeter. Note that even with the correction for viscosity, a region still exists on the calibration curve that is susceptible to variations in viscosity (Figure 11 [13]). The

point at which the alternate viscosity calibrations begin to diverge is known as the breakaway point. A calibration can still be used to the left of the breakaway point as long as the working fluid maintains a viscosity close to that of the calibration fluid. If the viscosity of the working fluid is expected to vary significantly, then the calibration should only be used to the right of the breakaway point. When selecting the flowmeter to use for a particular application, the applicable calibration region should be considered. If only the region to the right of the breakaway point can be used, then the flowmeter will have a smaller range of operation. This may necessitate the use of multiple sizes of flowmeters for an application in which a wide range of flow rates must be measured to a high degree of accuracy. This will be the case for turbine engine applications and will be discussed again later.

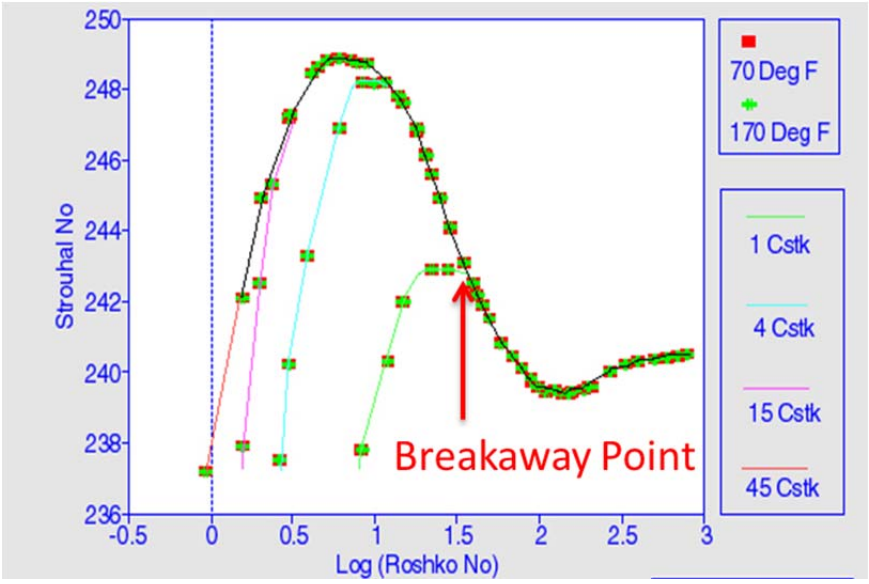

Figure 11. Strouhal Number vs. Roshko Number Curve [13]

3.2 FUEL FLOW CALCULATION METHOD

The method used to calculate fuel flow is taken from the SAE standard ARP 4990 [8] for turbine flowmeter fuel flow calculations. This standard utilizes the Strouhal vs. Roshko number relationship and accounts for differences between the operational fuel properties and the calibration fluid properties. Fuel flow was calculated using a routine called WFUELARP that is a subroutine within the Turbine Engine Test Analysis Standard program used at AEDC for gas turbine engine performance calculations. The ARP 4990 calculation method requires the following inputs:

FYFM	Flowmeter Frequency, Hz
AKFACTFM	Flowmeter calibration table, Strouhal no. vs. Roshko no.
TOP	Operational fluid temperature at flowmeter, °R
TCAL	Fluid Temperature during flowmeter calibration, °R
RD60F	Relative density of test fluid sample at 60°F referenced to water at 4°C in vacuo
TVIS	Temperature of fluid at viscosity VIS, °R
VIS	Viscosity of fluid sample at TVIS, centistokes
SLVIS	Slope of linearized viscosity versus temperature
POP	Operational fluid pressure at flowmeter, psia
PAMB	Ambient pressure around flowmeter during operation, psia
PCAL	Fluid pressure during calibration, psia
CALPHA	Fluid thermal expansion coefficient, 1/°F

CFTE	Flowmeter coefficient of linear thermal expansion, 1/°F
DIFM	Inner diameter of flowmeter, inches
CMOE	Modulus of elasticity of the flowmeter material, psi
XL	Wall thickness of the flowmeter, inches

The following parameters are useful outputs from the fuel flow calculation:

RHOOP	Fuel Density at operating conditions, lbm/U.S. Gallon
VISOP	Fuel viscosity at operating conditions, centistokes
CKOP	Flowmeter K-factor at operating conditions, pulses/gal
WF	Calculated fuel flow rate, lbm/hr

3.3 INSTALLED CONFIGURATION

The fuel flowmeters should be selected for the full range of fuel flow of the test article or other application. The calibration for a given size of flowmeter will only be usable over a certain range of flow rates. Often in turbine engine applications, the range of flow rates that are required is too wide for only one size of flowmeter to be able to adequately and safely measure. If the flowmeter is too large, the velocity through the flowmeter at low rates may not be high enough to spin the flowmeter rotor at an adequate rate to provide good measurement. Furthermore, if the viscosity of the operating fluid is expected to vary, the calibration will not be usable to the left of the breakaway point. On the other hand, if the flowmeter is too small, it may not be able to structurally handle the pressure loads and rotor velocity required to push the higher flow rates through the meter. A system that utilizes multiple ranges of flowmeters is desirable to

accurately and safely measure fuel flow for the entire operating range for the application.

A basic fuel flow measurement system for a turbine engine test cell is shown in Figure 12. The system is composed of a two flow measurement legs, a high leg and a low leg (more flow measurement legs can be added as needed). Each leg consists of two flowmeters in series. Utilization of two flowmeters allows for validation of the fuel flow data and is assumed to provide lower uncertainty than only one meter would provide. The fuel will always pass through the high range flowmeters (WFH1 and WFH2). The flow path downstream of the high range meters is governed by a control valve which can either force the fuel to pass through the low range flowmeters (WFL1 and WFL2) or allow the flow to bypass the low flowmeters.

The following instrumentation is critical for calculating accurate fuel flow and should always be included in the fuel flow measurement system:

- Flowmeter frequency, Hz
- Fuel Temperature (preferably upstream and downstream), ºR
- Fuel Pressure, psia

The fuel temperature and pressure measurements should be taken as close to the flowmeters as possible without impeding the flow quality entering the flowmeters. Ideally, the measurement package in the installed test configuration would be identical to the measurement package used in calibration. It will be shown later how differences between the calibration and installed configurations can add to the measurement uncertainty of the system.

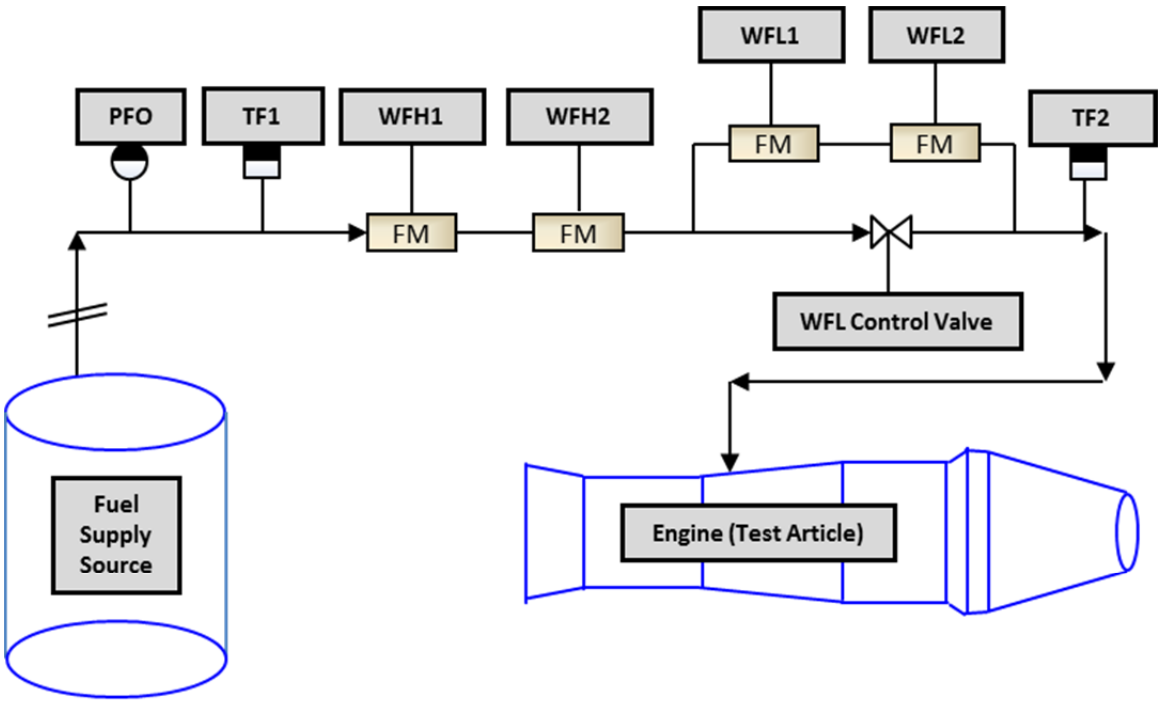

PFO	Operational fuel supply pressure, psia
TF1	Upstream operational fuel temperature, psia
TF2	Downstream operational fuel temperature, psia
WFH	High Range Flowmeter frequency signal, Hz
WFL	Low Range Flowmeter frequency signal, Hz

Figure 12. Fuel Flow Measurement System in a Turbine Engine Test Cell

4.0 FUEL FLOW MEASUREMENT UNCERTAINTY

4.1 STATEMENT OF SCOPE

Before diving into the analysis of fuel flow measurement uncertainty, it is imperative to determine the assumptions that we are making about the fuel flow measurement system and the data acquisition process.

4.1.1 Fuel Flow Measurement System Assumptions

The uncertainty analysis reported herein assumes that two flowmeters are calibrated in series with the same configuration that is used in the test installation. The calibration configuration should have at least 10 diameters length of piping upstream and downstream of the flowmeter leg to ensure that uniform flow quality is delivered to the inlet of the first flowmeter. The flow is calculated for each flowmeter, and the average of the two flow calculations is used for the total flow. In the test cell installed configuration, upstream and downstream temperature measurements should be taken as well as upstream pressure.

Pretest and post-test fuel samples are taken from the fuel batch that is used for a test. The samples are sent to a chemistry lab to have the properties analyzed (particularly density and viscosity at 60°F) for use in the fuel flow calculation.

4.1.2 Data Acquisition Process

The uncertainty reported herein assumes that the flow is fully stabilized and only applies to steady state data. A steady state data point is the average of ten seconds of data acquired at 10 samples per second. It is also assumed that the fuel flow data is taken only along the linear portion of the calibration curve to the right of the breakaway point.

4.2 SOURCES OF ERROR

Each of the inputs to the ARP 4990 fuel flow algorithm introduces uncertainty to fuel flow measurement. The simplest method to perform an uncertainty analysis for a complex system is to first determine the influence coefficients for each of the error sources, then determine the elemental uncertainty for each error source, while focusing more on the sources of error that have large influence coefficients. In most engineering applications, only 3 or 4 error sources dominate the other error sources. Parameters with small influence coefficients can be assigned conservative uncertainties that are likely to be overestimates of their actual error. The combined uncertainty and the percent contribution from each error source are then calculated using the influence coefficients and the elemental uncertainties. If all of the large contributors to the combined uncertainty were evaluated with realistic elemental uncertainties, then the analysis is complete. If any parameters that were assigned a conservative uncertainty estimate turn out to be a large contributor, they must then be reevaluated. Figure 13 is an uncertainty analysis flow chart.

4.2.1 Influence Coefficient Analysis

The first step in the uncertainty analysis is to determine the influence coefficient for each of the error sources. The dithering method described in Section 5.2.2 (a numerical version of the TSM) was used to calculate relative influence coefficients for each of the fuel flow calculation inputs. A relative influence coefficient describes the influence of a variable on the dependent parameter in terms of percent. For example, a relative influence coefficient of 1 means that a 1% change in the variable results in a 1% change in the dependent parameter. Table 1 lists the relative influence coefficient for each error source.

Table 1. Relative Influence Coefficients for Fuel Flow Calculation Inputs

Variable Name	Description	IC
FYFM	Flowmeter Frequency	1
AKFACTFM	Flowmeter Calibration Table	1
TOP	Operational Fuel Temperature at Flowmeter	-0.27
TCAL	Fluid Temperature at Flowmeter Calibration	-0.015
RD60F	Relative Density of Fuel at 60°F Referenced to Water at 4°C in Vacuo	1
TVIS	Temperature of Fuel at Viscosity, VIS	0.01
VIS	Viscosity of Operational Fuel at TVIS	0.002
SLVIS	Linearized Slope of Viscosity vs. Temperature	-0.0002
FTYPE	Fluid Type (4 for JP-4, 8 for JP-8/Jet-A)	N/A
POP	Operational Fuel Pressure at Flowmeter	0.0003
PAMB	Ambient Pressure around Flowmeter During Operation	<< 0.0001
PCAL	Fluid Pressure during Calibration	<< 0.0001
CALPHA	Fluid Thermal Expansion Coefficient	-0.0053
CFTE	Flowmeter Coefficient of Linear Thermal Expansion	<< 0.0001
DIFM	Inner Diameter of Flowmeter	<< 0.0001
CMOE	Modulus of Elasticity of Flowmeter Material	<< 0.0001
XL	Wall Thickness of Flowmeter	<< 0.0001

Significant Contributor to Total Fuel Flow Uncertainty
Insignificant Contributor to Total Fuel Flow Uncertainty

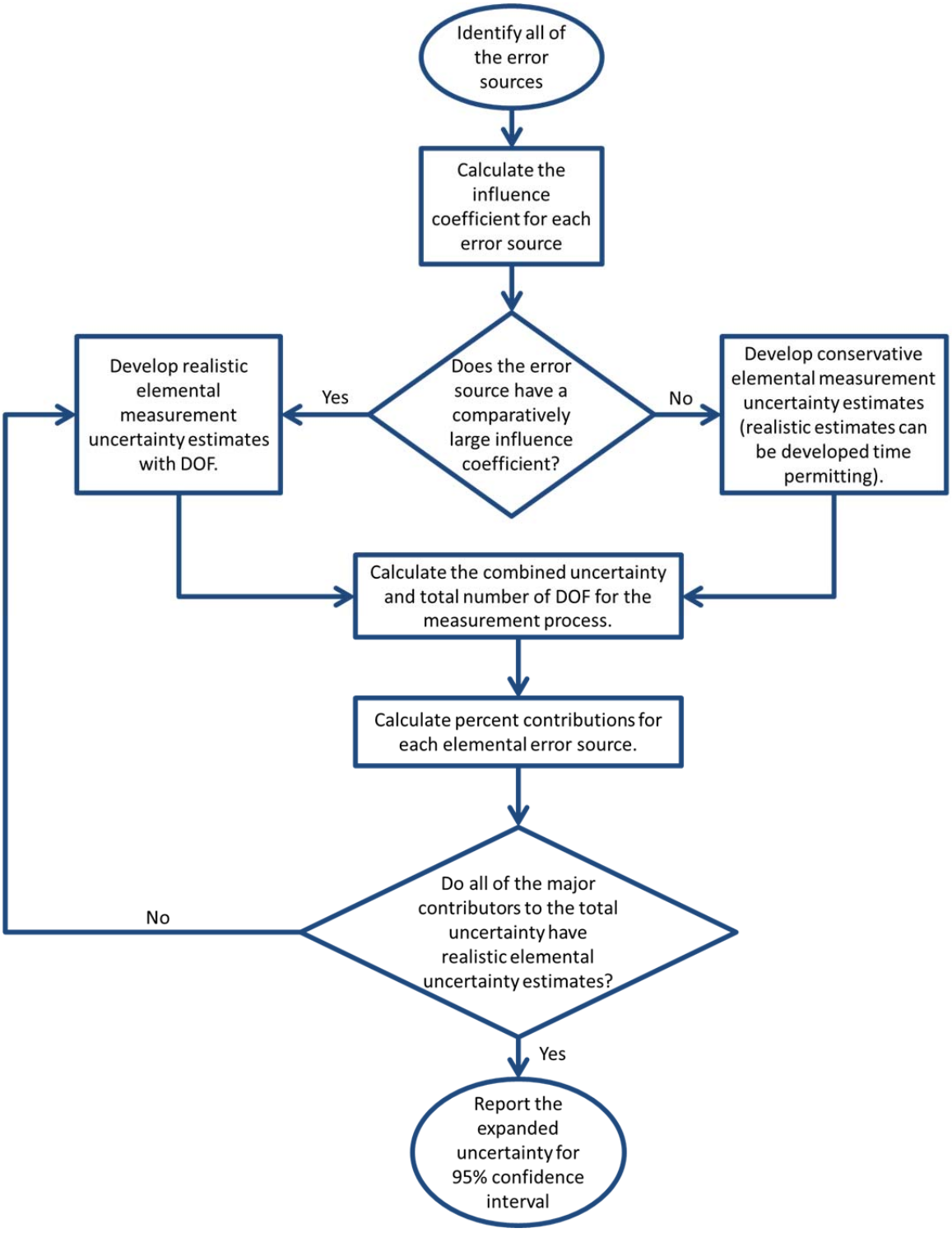

Figure 13. Uncertainty Calculation Methodology

4.2.2 Uncertainty on High Influence Error Sources

4.2.2.1 Flowmeter Calibration Uncertainty

The flowmeters are calibrated at several Roshko numbers over the overall Roshko range of the meter. The uncertainty of a given flowmeter calibration can be estimated from the calibration history. A minimum of two calibrations are taken when a flowmeter is initially acquired, and the flowmeters are recalibrated once every 12 months throughout the life of the meter. Assuming that no significant drift in the calibration is noted, the average of all of the calibrations will provide the most reliable calibration to use in the fuel flow calculation. The standard deviation of the Strouhal numbers at each of the Roshko levels along the calibration gives an estimate of the uncertainty in the calibration. This method takes into account the uncertainty inherent in the flowmeter calibration bench and the flowmeter repeatability during calibration. Figure 14 and Figure 15 show the calibration histories for two flowmeters in series. Table 2 lists the standard deviation of the Strouhal numbers at each Roshko level. Observe that the Strouhal number standard deviation is approximately equal for each Roshko number along the calibration. For the sake of being conservative, the largest standard deviation will be used for the uncertainty of the average flowmeter calibration that is used in the fuel flow calculation. This yields an uncertainty of 0.11% for flowmeter 1 and 0.05% for flowmeter 2.

The number of degrees of freedom for the calibration is determined by the number of data points used to determine the calibration. The fuel flow calculation

calculates a Roshko number using the as-tested fuel properties, then interpolates a value for the as-tested Strouhal number from the calibration table. For a linear interpolation (a type of curve fit) the number of DOF is equal to two less than the number of points in the curve fit [1, 2, 4]. If the calibration table used in the program is actually the average of n number of historical calibrations, then the number of DOF for the Strouhal number equals 2n-2. This is demonstrated in Figure 16. In this example, 5 historical calibrations are averaged to obtain a single calibration table. The number of DOF for this example is therefore 8.

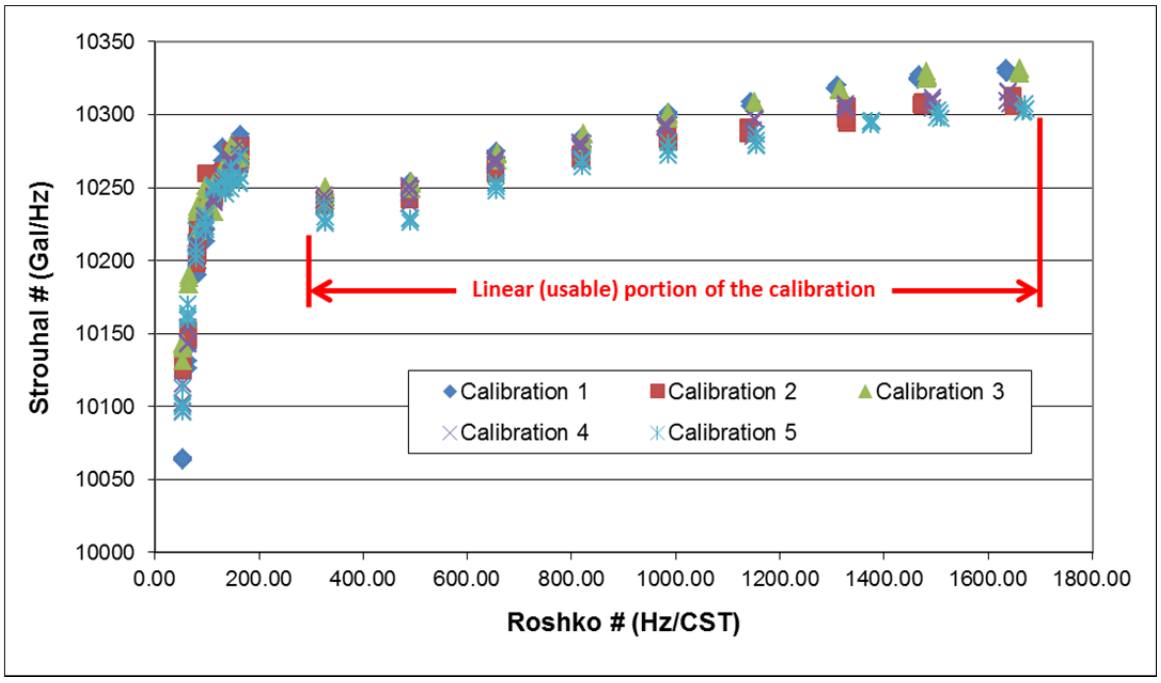

Figure 14. Flowmeter 1 Calibration History

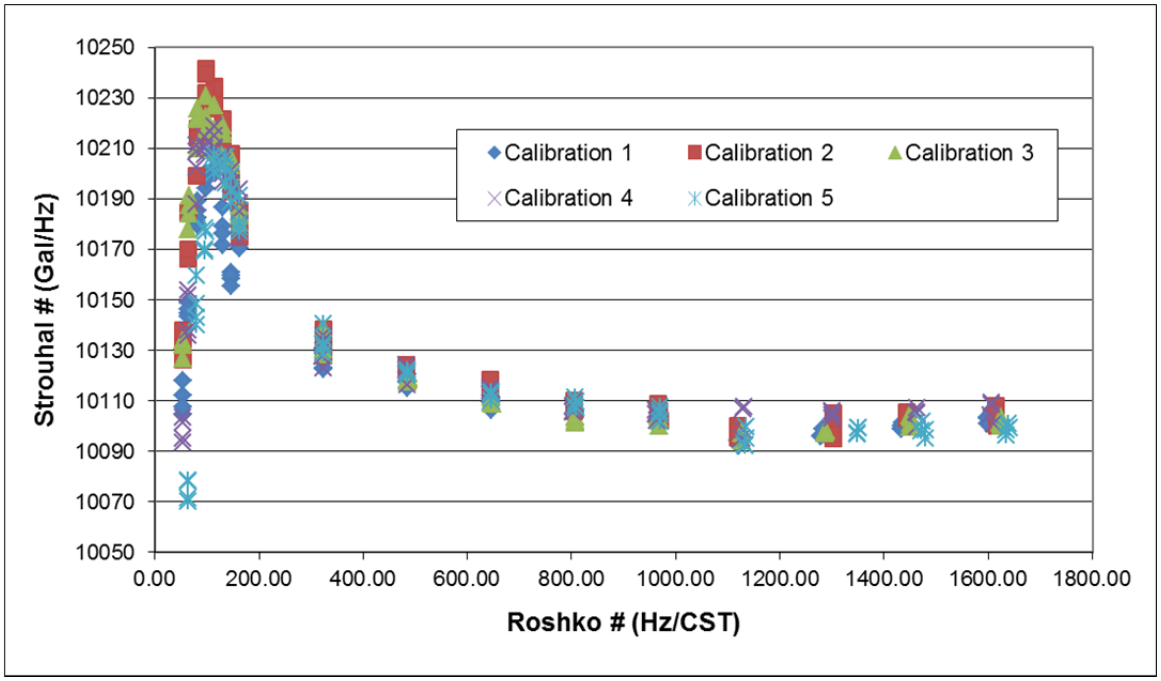

Figure 15. Flowmeter 2 Calibration History

Table 2. Flowmeter Calibration Standard Deviations

Flowmeter 1			Flowmeter 2		
Average Roshko	Average Strouhal	Strouhal STDEV (%)	Average Roshko	Average Strouhal	Strouhal STDEV (%)
1651	10317	0.110	1616	10103	0.035
1484	10313	0.107	1454	10102	0.032
1331	10307	0.095	1304	10099	0.035
1148	10296	0.108	1126	10097	0.042
985	10290	0.092	967	10104	0.022
820	10277	0.068	806	10106	0.026
655	10265	0.080	646	10112	0.027
491	10244	0.088	485	10120	0.026
327	10239	0.061	323	10131	0.050
164	10271	0.090	162	10182	0.059
147	10269	0.078	146	10191	0.169
132	10258	0.070	131	10203	0.147
114	10246	0.053	114	10214	0.105
98	10231	0.116	98	10208	0.218
81	10210	0.137	81	10193	0.268
65	10157	0.181	65	10144	0.390
53	10107	0.267	53	10085	0.684

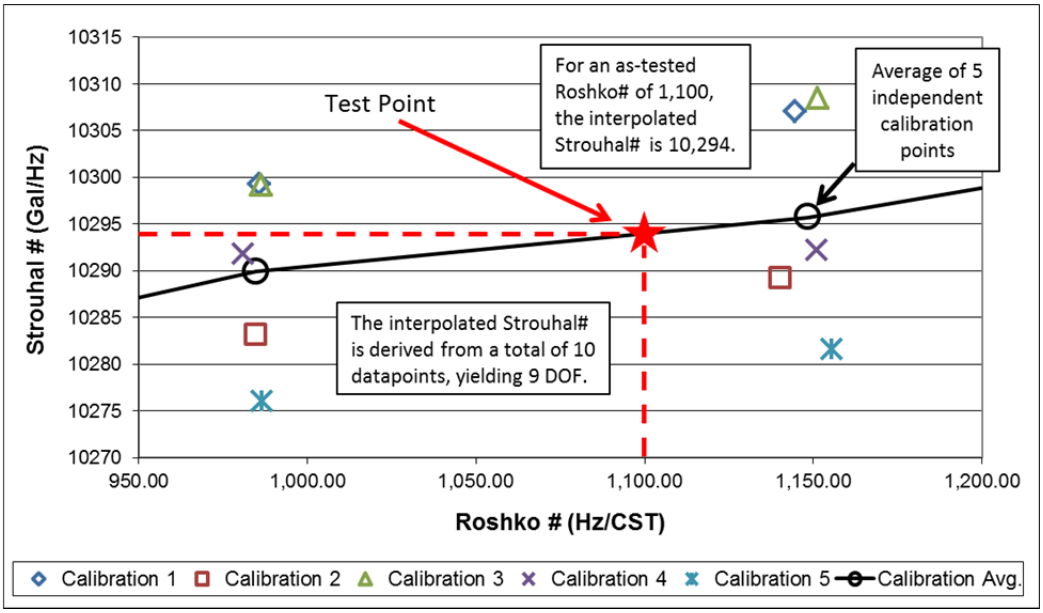

Figure 16. Strouhal Number Interpolation with 8 DOF

4.2.2.2 Flowmeter Frequency

The uncertainty for the flowmeter frequency measurement is often provided by the manufacturer of the flowmeter. However, uncertainty figures provided by manufacturers are often difficult to interpret and may not include additional sources of error when the flowmeter is installed in the measurement system. Therefore, the uncertainty for the flowmeter should be evaluated using the test data. The fuel flow measurement systems in the turbine test cells at AEDC utilize two flowmeters in series, as shown in Figure 12. The uncertainty of the frequency measurement for both of the flowmeters can be estimated using the difference between the frequency measurements. The percent difference between the flowmeter frequencies for a test project is shown in Figure 17. The standard deviation of the delta can be used as the random uncertainty of the

frequency measurement. The random uncertainty of the frequency for this project is 0.074% of reading. A probability plot is commonly used to check a data set for normality. Figure 18 demonstrates the high degree of normality of the percent difference between the two flowmeters shown in Figure 17.

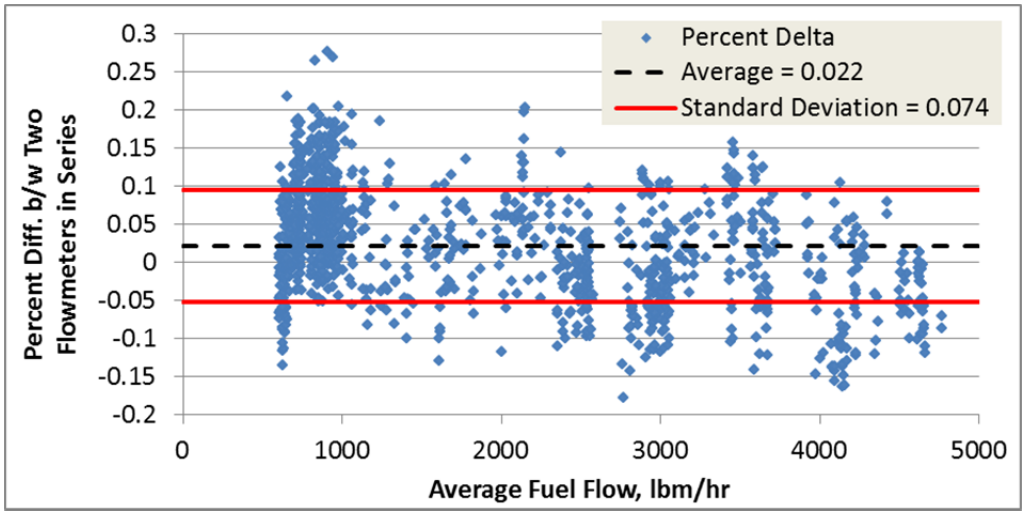

Figure 17. Percent Difference between Two Flowmeters in Series

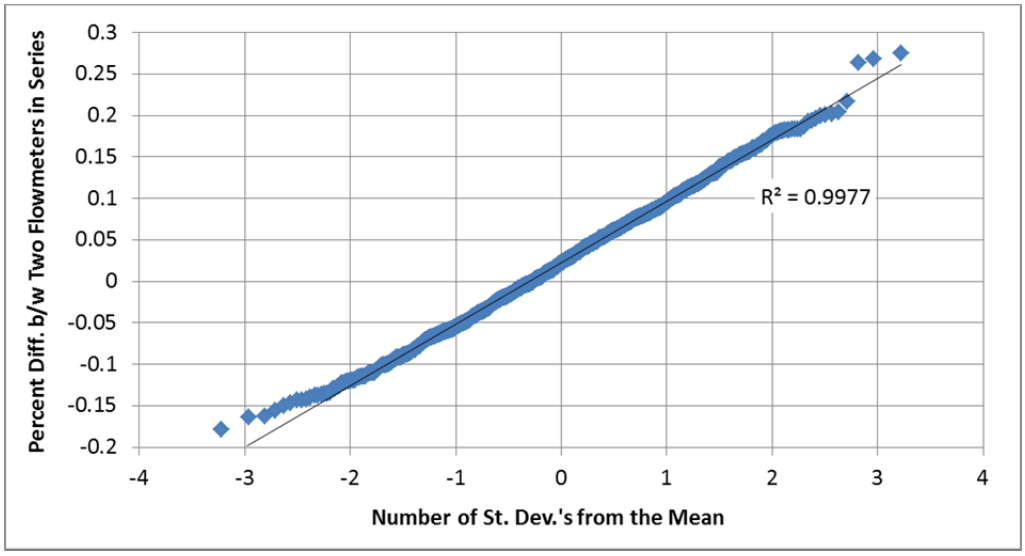

Figure 18. Normal Probability Plot for Flowmeter Frequency

The average delta cannot be used as the systematic uncertainty of the frequency measurement, because some difference is expected due to differences in the meters. These differences are accounted for in the flowmeter calibration. The systematic uncertainty for the data processing system was provided by the instrumentation engineer for this project and was 0.0005%.

The final elemental uncertainties associated with the flowmeter frequency parameter are 0.08% random uncertainty and 0.001% systematic uncertainty. The number of degrees of freedom associated with the random and systematic uncertainties is much greater than 30. For the purpose of this analysis, the DOF for any particular uncertainty component will be limited to 100. These uncertainties will be propagated to fuel flow in Section 4.3.

4.2.2.3 Fuel Density

Pre-test and post-test fuel samples are taken from the fuel batch that is used for a particular test. The samples are sent to a chemistry lab to be analyzed for density, viscosity, and other properties that may be germane to the test. After the fuel analysis reports are received, the pre- and post-test density and viscosity values at 60°F are averaged and used to post-process the test data. A log of the pre- and post-test relative density can be used to estimate the uncertainty of the average density used in the data post-processing.

Figure 19 shows a fuel sample relative density log from a particular test program with 24 tests. Figure 20 shows the percent difference between the pre- and post-test relative densities measured at the chemistry lab at 60°F for the test

program. The standard deviation of these percent differences is the random uncertainty of the fuel flow calculation input, RD60F. This random uncertainty accounts for errors in the chemistry lab density measurement, as well as fuel property variations within a batch of fuel used for a test. For the data shown in Figure 20, the standard deviation of the pre- to post-test density shift is 0.04%.

Systematic errors in the density meter at the AEDC chemistry lab can also be a potential source of significant error. Regular tests are performed on the density meter to verify that it remains within the specified tolerance (which is 0.08%) by measuring the density of a calibration fluid with a "known" density at 60°F. The results of these verification tests over a long period of time can be used to determine the systematic uncertainty of the density meter. Figure 21 shows the history of the density meter verification tests over a period of 13 months. The systematic uncertainty of the chemistry lab density meter can be estimated by taking the difference between the average of the verification test results and the certified value of the test fluid. Data over the 13 month span shown in Figure 21 indicates that the systematic uncertainty of the density meter is 0.01% of reading. As was previously stated, the random uncertainty of the density meter is inherently included in the uncertainty estimate from the pre- and post-test fuel samples. The final elemental uncertainties associated with fuel density are 0.04% random uncertainty and 0.01% systematic uncertainty. The number of degrees of freedom (n-1) associated with the random uncertainty is 19, and number of degrees of freedom for the systematic uncertainty is 31. These uncertainties will be propagated to fuel flow in Section 4.3.

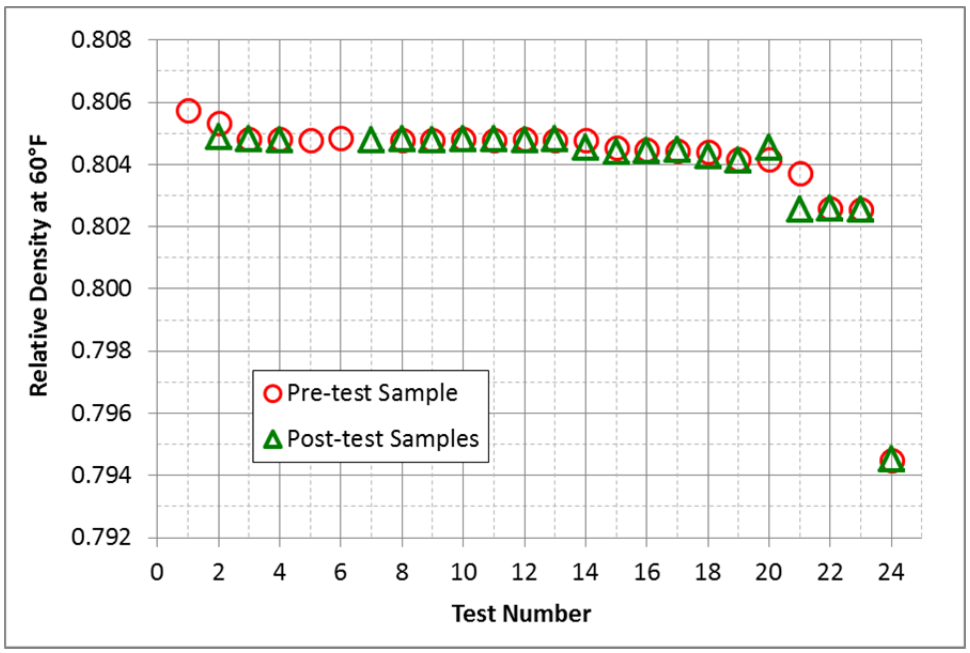

Figure 19. Example of a Fuel Sample Density Log

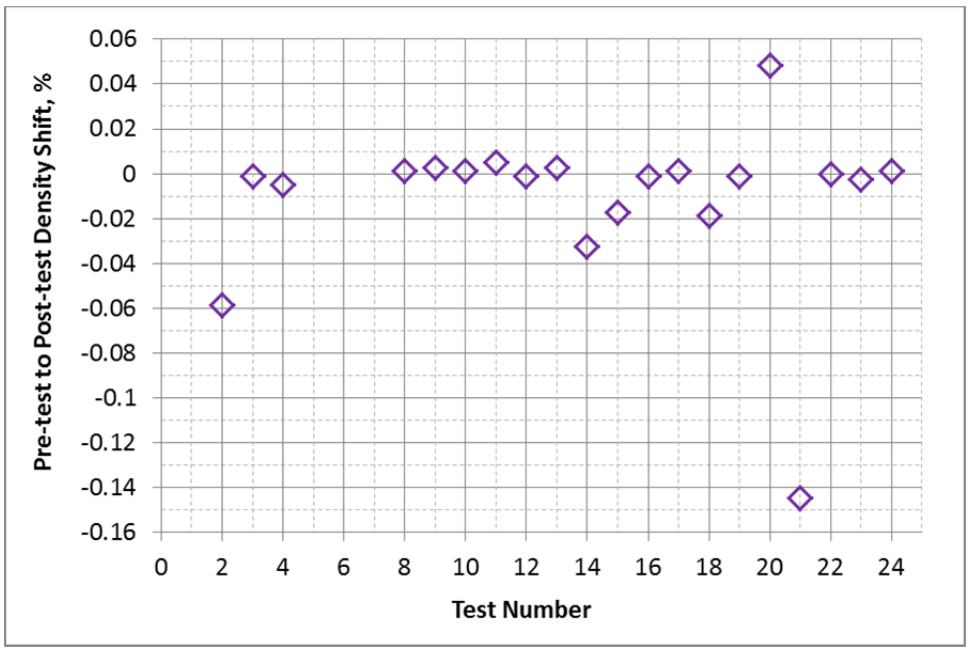

Figure 20. Percent Difference between Pre- and Post-Test Fuel Sample Relative Density

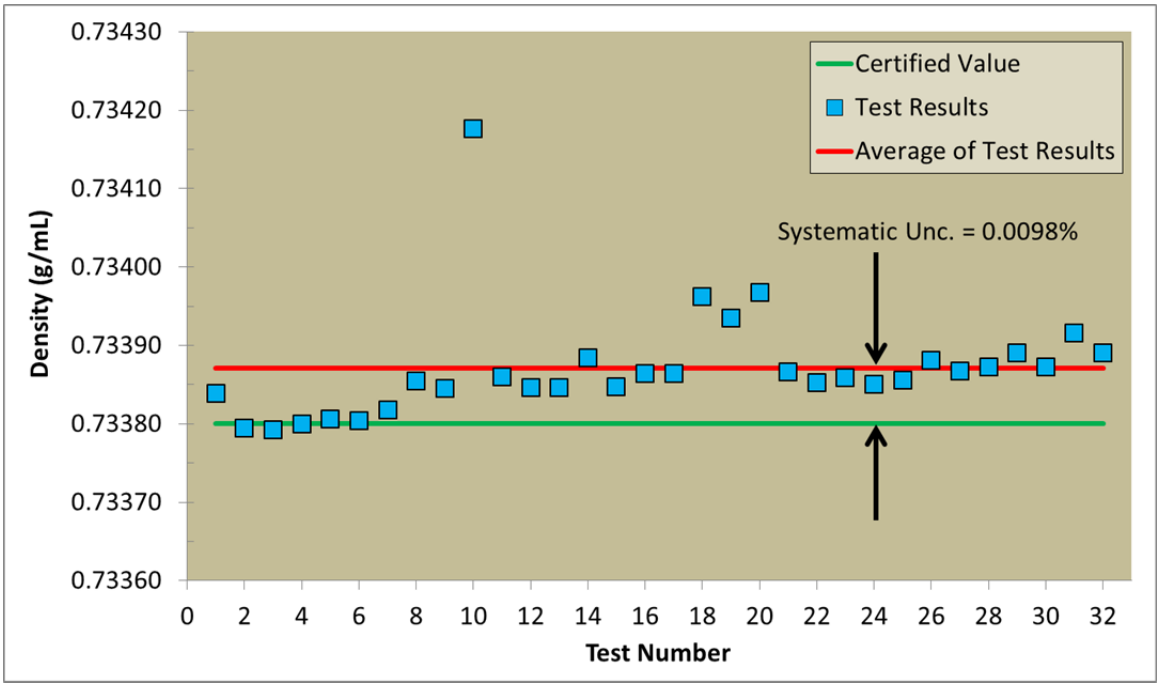

Figure 21. AEDC Chem Lab Density Verification History

4.2.2.4 Operational Fuel Temperature

The operational fuel temperature is measured using two thermocouples: one located upstream of the first flowmeter in the system and one located downstream of the final flowmeter in the system, as shown previously in Figure 12. The average of the two thermocouples is used as the fuel temperature input for the fuel flow calculation. The uncertainty for the thermocouples at AEDC is provided by the instrumentation engineer who analyzes the thermocouple calibrations and ensures that the repeatability is within the manufacturer's specification. The random and systematic uncertainties determined by the instrumentation engineer for the temperature measurements are 0.028°F and

1.27°F, respectively. However, the manufacturer-supplied uncertainty will only account for the uncertainty in the measurement itself and will take into account temperature variation from the first flowmeter to the last flowmeter.

Test data (similar to the data shown in Figure 22) can be used to estimate the uncertainty due to spatial temperature variations from the inlet to the outlet of the fuel flow measurement system. Due to differences in the temperature distribution at different levels of fuel flow, the temperature uncertainty due to spatial variations was evaluated in two ranges, 0-1200 lbm/hr and 1200-5000 lbm/hr. The random and systematic temperature uncertainties due to spatial variation are shown in Figure 22.

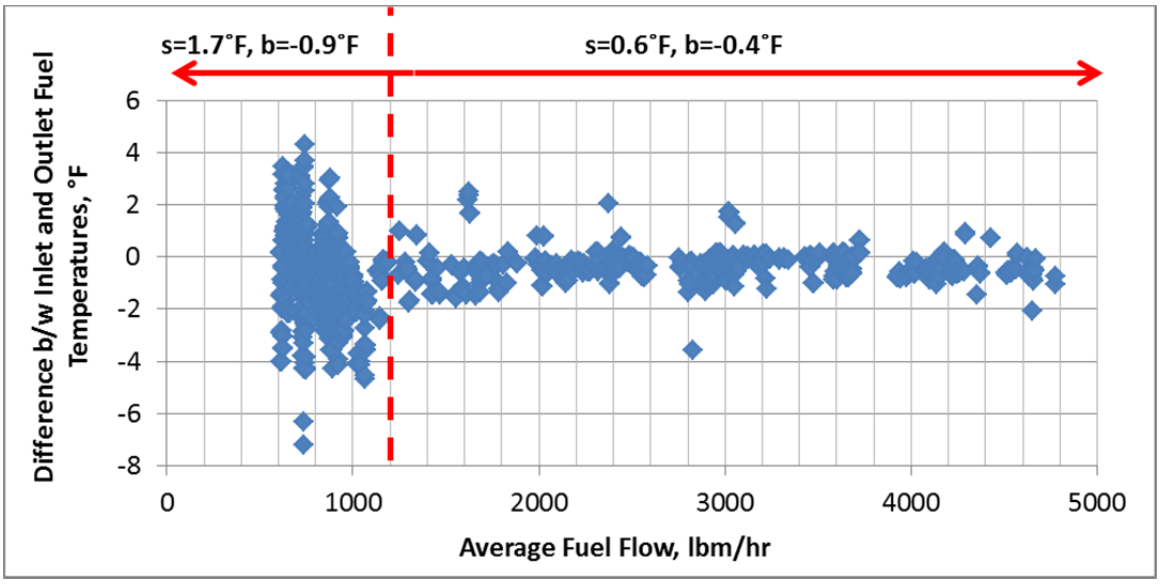

Figure 22. Random and Systematic Uncertainty of Inlet and Outlet Temperatures due to Spatial Variation

The total uncertainty for the fuel temperatures are the root-sum-square of the instrumentation system uncertainty and the spatial variation uncertainty. The total random and systematic uncertainty for the operational fuel temperature is shown in Table 3. The number of degrees of freedom associated with the random and systematic uncertainties is much greater than 30. For the purpose of this analysis, the DOF for any particular uncertainty component will be limited to 100. These uncertainties will be propagated to fuel flow in Section 4.3.

Table 3. Random and Systematic Uncertainty for Operational Fuel Temperature

Fuel Flow Range (lbm/hr)	Random Uncertainty (˚F)			Systematic Uncertainty (˚F)		
	Instrument	Spatial Variation	Total	Instrument	Spatial Variation	Total
0 - 1200	0.028	1.7	1.7	1.27	0.9	1.56
1200 - 5000	0.028	0.6	0.6	1.27	0.4	1.33

4.2.3 Uncertainty on Low Influence Error Sources

The remaining parameters that are inputs into the fuel flow calculation have relatively insignificant influence coefficients compared to the parameters considered in section 4.2.2. The elemental uncertainty for the remaining parameters will be evaluated conservatively. It will be shown in Section 4.3 that the uncertainty for these parameters has no impact on the combined fuel flow uncertainty, even with conservative uncertainty estimates.

4.2.3.1 Viscosity Related Parameters

The parameter VIS is the viscosity at a selected temperature (TVIS) that is measured from the pre- and post-test fuel samples that are sent to the chemistry lab. For convenience, TVIS is typically 60ºF, so that the density and viscosity are evaluated at the same temperature at the chemistry lab.

The method used to evaluate the uncertainty of the fuel relative density is also used to assess the uncertainty of the viscosity. Figure 23 and Figure 24 show a fuel sample viscosity log and the percent difference between the pre- and post-test viscosities found in the log. The standard deviation of these percent differences is the random uncertainty of the fuel flow calculation input, VIS. This random uncertainty accounts for the uncertainty of the chemistry lab viscosity measurement as well as the random variation in any given batch of fuel used during a test. For the viscosity log shown, the standard deviation of the pre- to post-test deltas is 0.5%. The systematic uncertainty of VIS is estimated using the chemistry lab viscosity meter verifications, similar to the method performed for density. Figure 25 shows the history of the density meter verification tests over a period of 13 months. The systematic uncertainty of the chemistry lab viscosity meter can be estimated by taking the difference between the average of the verification test results and the certified value of the test fluid. As shown in Figure 25, the systematic uncertainty of the viscosity meter is 0.02% of reading.

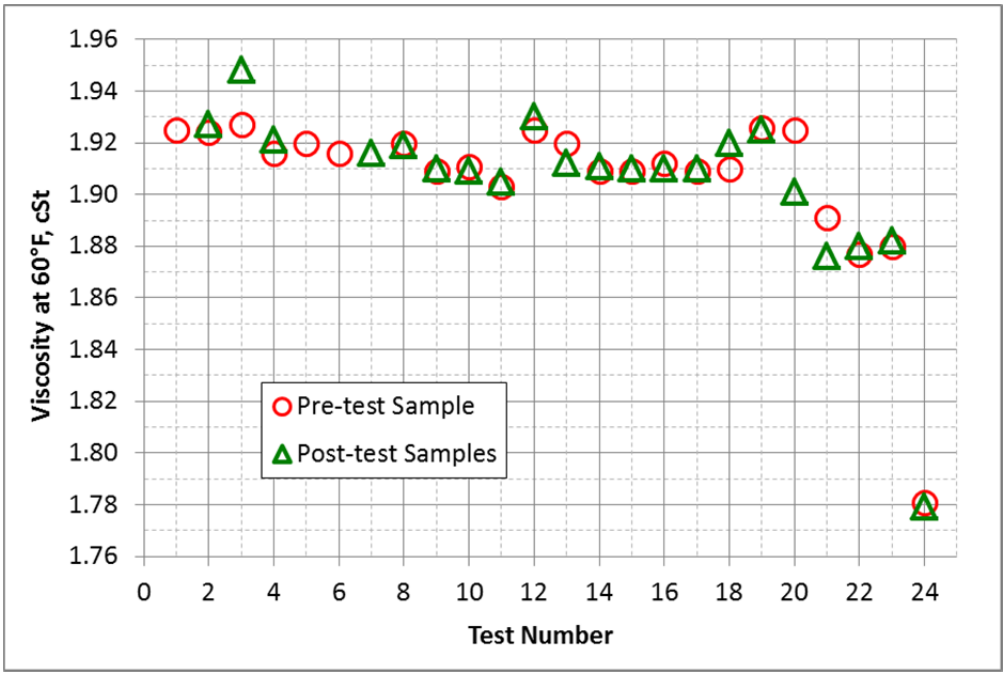

Figure 23. Example of a Fuel Sample Viscosity Log

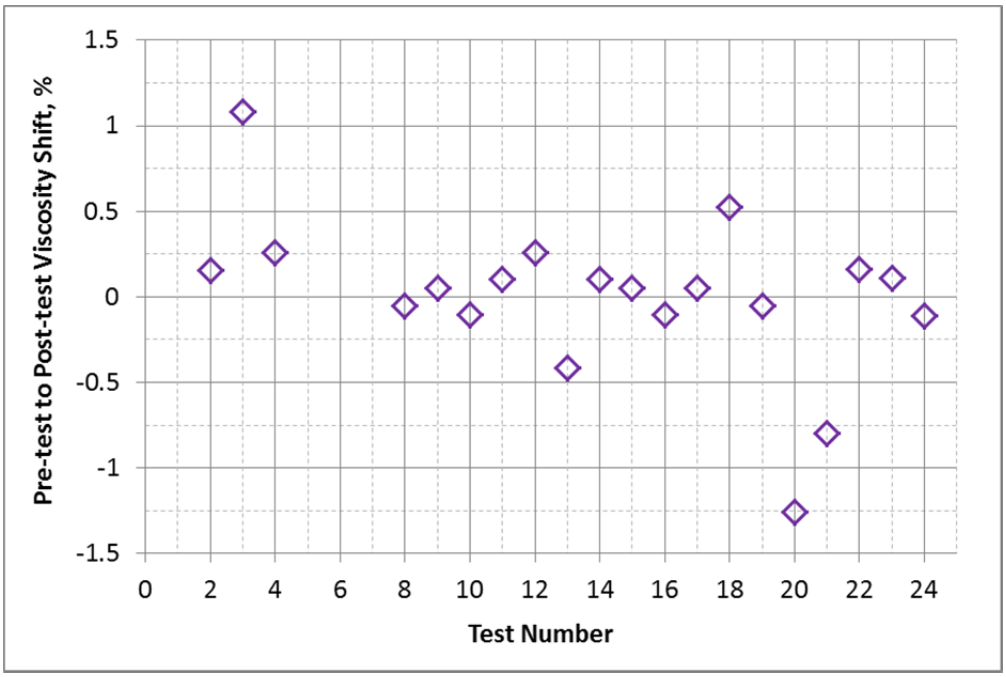

Figure 24. Percent Difference between Pre- and Post-Test Fuel Sample Viscosity

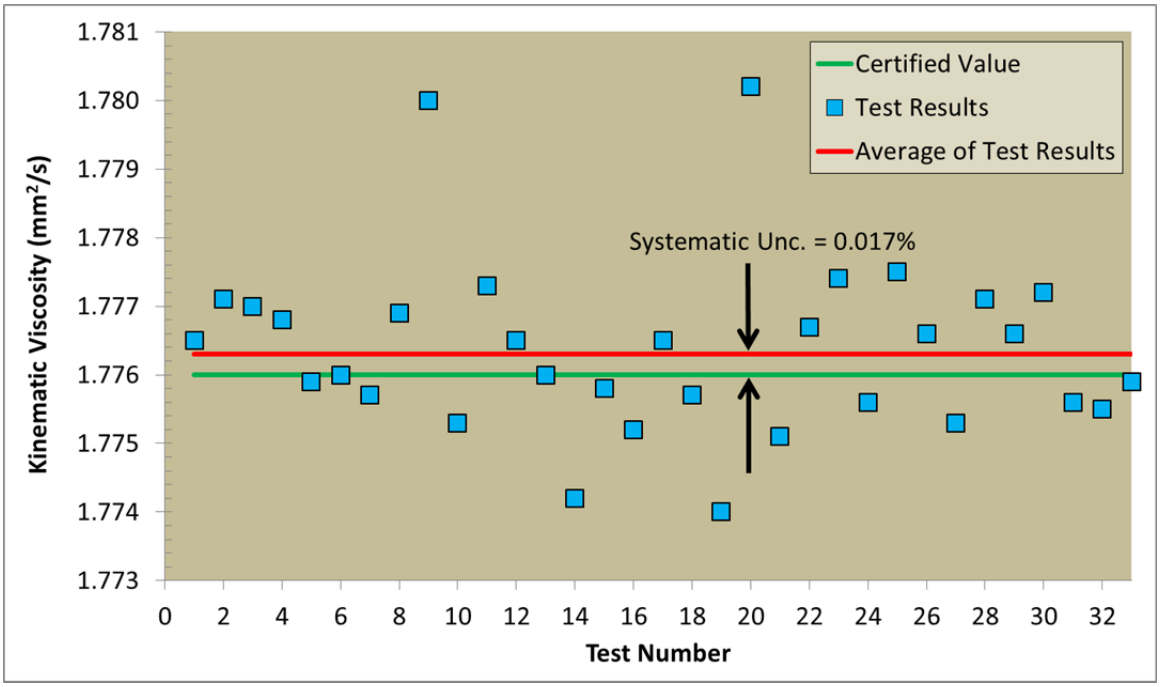

Figure 25. AEDC Chem Lab Viscosity Verification History

The uncertainty of TVIS is inherently included in the uncertainty of VIS. Any random variation in TVIS would necessarily result in random variation in VIS, and any systematic shift in TVIS would necessarily result in a systematic shift in VIS. Thus, the random and systematic uncertainty estimates for VIS will include the uncertainty of TVIS.

The value used for the slope of the viscosity vs. temperature correlation (SLVIS) is typically a standard value for the type of fuel that is being used for the test. This value is assumed to be correct within 5% of the true slope. This uncertainty estimate is the 95% coverage interval, so the 1-sigma uncertainty estimate for SLVIS is 2.5% with infinite degrees of freedom. The number of degrees of freedom for any elemental uncertainty is limited to 100 herein.

4.2.3.2 Additional Temperature and Pressure Corrections

The temperature and pressure of the calibration fluid (TCAL and PCAL) used during the flowmeter calibrations is used as the baseline temperature and pressure for calculating the Strouhal and Roshko numbers. The pressure of the fuel going through the flowmeter (POP) and the atmospheric ambient pressure (PAMB) are used to correct the operational fuel properties to the conditions during the calibration. The temperature and pressure corrections are described in detail in Ref. 8.

The uncertainty of TCAL and PCAL should be quoted by the calibration authority (at AEDC, the calibrating authority is the PMEL). At the AEDC PMEL, the uncertainty on TCAL is quoted as 0.26%. The PMEL did not provide a quote for the uncertainty on PCAL, so a relatively large uncertainty value of 1% is assumed for the uncertainty. Since the errors in TCAL and PCAL will become fossilized in the calibration, their respective uncertainties are categorized as systematic uncertainty.

The uncertainties of PAMB and POP are quoted by the instrumentation engineer for the pressure measurement system in the test cell. For the purposes of this discussion, the uncertainty on POP and PAMB are shown in Table 4.

Table 4. Uncertainty for POP and PAMB

Parameter	Systematic Unc. (psia)	Random Unc. (psia)
POP	0.038	0.02
PAMB	0.0032	0.0012

4.2.3.3 Coefficient of Thermal Expansion

The coefficient of thermal expansion (CALPHA) of the fuel at the reference temperature TCAL is used in conjunction with TOP to determine a volume correction factor to account for the difference in density when the fuel temperature is at TOP versus TCAL. The value of CALPHA most often used for the fuel flow calculation is 0.00051 for JP-8 and Jet-A fuels. Checks are occasionally performed on fuel arriving at AEDC to ensure that thermal expansion properties of the fuel are acceptable. It is the author's experience that the value of CALPHA rarely exceeds 0.00051 +/- 2%. The uncertainty at the 1-standard deviation level for CALPHA is then 1%, with degrees of freedom limited to 100.

4.2.3.4 Flowmeter Physical Dimensions and Material Properties

The inner diameter (DIFM), wall thickness (XL), coefficient of linear thermal expansion (CFTE), and modulus of elasticity (CMOE) are used in conjunction with the operational temperature and pressure to correct the Strouhal number for dimensional changes in the flowmeter between the operating conditions and the calibration conditions. It is assumed that the uncertainty on each of these parameters is 5%. While the true error on each of these parameters is likely far less than 5%, it will be shown that 5% uncertainty has no significant impact on the final fuel flow uncertainty. The 1-standard deviation uncertainty interval that is used for each of these parameters is therefore 2.5%.

4.3 COMBINED FUEL FLOW UNCERTAINTY

4.3.1 Taylor's Series Method

Once all of the error sources have been identified and a level of uncertainty has been determined for all of the inputs to the fuel flow calculation, the uncertainties can be propagated to fuel flow and the combined uncertainty can be determined. A summary of the uncertainties for the elemental error sources is shown in Table 5. Using the influence coefficients shown in Table 1 and the elemental uncertainties from Table 5, the combined fuel flow uncertainty is calculated using the U_{95} method (Eq. 19). For the uncertainty of an individual flowmeter, the influence coefficient of the flowmeter frequency on fuel flow is equal to one. However, for the average of two flowmeters in series, the influence coefficient for each of the flowmeter frequencies and the flowmeter calibrations is one half. All other influence coefficients remain the same for the average of the two flowmeters. When the combined uncertainty equation is applied, the combined uncertainty for average fuel flow at the one standard deviation level is 0.12% of reading. The combined number of degrees of freedom for average fuel flow, calculated using the Welch-Satterthwaite formula (Eq. 18), is 131, substantially more than the 30 degrees of freedom needed to make the large sample assumption. Applying a Student's t-value of 2 for the 95% confidence interval yields 0.25% uncertainty for average fuel flow. The calculations used to derive the combined uncertainty and the number of combined degrees of freedom are shown in Table 6.

Table 5. Fuel Flow Elemental Uncertainty Summary

Fuel Flow Elemental Error Sources	Systematic (Bias) Uncertainty, b			Random (Precision) Uncertainty, s			Method Used to Estimate Uncertainty
	+/- units	+/- %Rd	DOF	+/- units	+/- %Rd	DOF	
Flowmeter Calibration							
Calibration for Meter 1		0.11	8				Standard deviation of several calibrations
Calibration for Meter 2		0.05	8				
Cal. Fluid Temp.		0.26	100				Quoted value from AEDC PMEL
Cal. Fluid Pressure		1.00	100				Estimated value: negligible influence on total uncertainty
Operational Fuel Properties							
Density		0.01	31		0.04	19	Random unc. is the stand. dev. of the deltas between pre- and post-test fuel samples. Systematic unc. is the estimated from the chem. lab. meter verifications.
Viscosity		0.02	31		0.5	19	
Temperature at Viscosity							Temperature uncertainty accounted for in viscosity uncertainty
Viscosity vs. Temp. Slope		2.50	100			100	Estimated uncertainty of the linear regression. This term has a negligible impact on total
Fuel Thermal Expansion Coefficient		1.00	100				Estimated uncertainty based on experience
Fuel Temperature	1.33		100	0.6		100	RSS of the instrumentation uncertainty quote provided by instrumentation engineer and the delta between the up- and downstream temperature measurements
Fuel Pressure	0.038		100	0.02		100	Provided by the instrumentation engineer
Flowmeter System							
Ambient Pressure	0.0032		100	0.0012		100	Provided by the instrumentation engineer
Inner Diameter		2.50	100				Estimated value: negligible impact on total uncertainty
Modulus of Elasticity		2.50	100				Estimated value: negligible impact on total uncertainty
Wall Thickness		2.50	100				Estimated value: negligible impact on total uncertainty
Thermal Expansion Coefficient		2.50	100				Estimated value: negligible impact on total uncertainty
Data Acquisition							
Flowmeter Frequency		0.001	100		0.08	100	Estimated from the deltas b/w the up- and downstream meters

Table 6. Summary of Combined Uncertainty Calculation Using TSM

Fuel Flow Rate =	WF1 = 4640 pph
	WF2 = 4642 pph
	Average = 4641 pph

Parameter Inputs		Influence Coefficient Calculation					Elemental Uncertainties							Degrees of Freedom	
			Perturbated Output				Systematic		Random					Welch-Satterthwaite Eq.	
Name	Value	Pert. Input (Input * 1.001)	WF1 (Pert)	WF2 (Pert)	Avg	IC_i	b_i (%)	$\nu_{b,i}$	s_i (%)	$\nu_{s,i}$	Comb. Unc. (u_i)	$(IC_i*u_i)^2$	% Contri-bution	Numerator	Denominator
FYFM (1)	2037.0	2039.010974	4644.5		4643.5	0.497	0.001	100	0.08	1.00E+02	0.081	0.0016215	11.112	0.001581933	2.50173E-08
FYFM (2)	1998.3	2000.274176		4647.1	4643.5	0.500	0.001	100	0.08	1.00E+02	0.081	0.00164	11.239	0.001600024	2.55928E-08
Cal Table (1)	Cal 1	Cal 1 (Pert)	4635.3		4638.9	-0.499	0.11	8			0.110	0.0030173	20.678	0.003017309	1.13802E-06
Cal Table (2)	Cal 2	Cal 2 (Pert)		4637.8	4638.9	-0.500	0.05	8			0.050	0.0006241	4.277	0.000624093	4.86865E-08
TOP	555.1585	555.7136585	4638.6	4641.2	4639.9	-0.283	0.24	100	0.11	1.00E+02	0.263	0.0055414	37.976	0.005533905	2.20184E-07
TCAL	530	530.53	4639.8	4642.4	4641.1	-0.016	0.26	100			0.260	1.693E-05	0.116	1.69347E-05	2.86783E-12
RD60F	0.79451	0.79530451	4644.6	4647.1	4645.8	0.999	0.01	31	0.04	19	0.042	0.0017602	12.063	0.001696322	1.34476E-07
TVIS	520	520.52	4640.0	4642.5	4641.2	0.023							0.000		
VIS	1.78	1.78178	4639.9	4642.5	4641.2	0.005	0.02	31	0.5	19	0.501	6.341E-06	0.043	6.32625E-06	2.09967E-12
SLVIS	-3.523	-3.526523	4639.9	4642.5	4641.2	-1.5E-03	2.50	100			2.500	1.372E-05	0.094	1.37211E-05	1.88268E-12
POP	63.56098	63.62454098	4639.9	4642.5	4641.2	0.000	0.059785	100	0.03	100	0.068	1.029E-09	0.000	1.01583E-09	6.81339E-21
PAMB	4.35514	4.35949514	4639.9	4642.5	4641.2	-7.2E-07	0.073476	100	0.03	100	0.079	3.212E-15	0.000	3.16892E-15	7.87118E-32
PCAL	60	60.06	4639.9	4642.5	4641.2	-9.9E-06	1.00	100			1.000	9.767E-11	0.000	9.7672E-11	9.53983E-23
CALPHA	0.00051	0.00051051	4639.8	4642.4	4641.1	-0.019	1.00	100			1.000	0.0003468	2.377	0.000346832	1.20293E-09
CFTE	0.00001	0.00001001	4639.9	4642.5	4641.2	7.5E-04	2.50	100.00			2.500	3.528E-06	0.024	3.52799E-06	1.24467E-13
DIFM	0.625	0.625625	4639.9	4642.5	4641.2	2.2E-06	2.50	100.00			2.500	3.047E-11	0.000	3.04744E-11	9.28691E-24
CMOE	30000000	30030000	4639.9	4642.5	4641.2	-2.2E-06	2.50	100.00			2.500	3.041E-11	0.000	3.04136E-11	9.24987E-24
XL	0.378	0.378378	4639.9	4642.5	4641.2	-2.2E-06	2.50	100.00			2.500	3.041E-11	0.000	3.04136E-11	9.24987E-24

Uncertainty, U95 = $2*[\sum(IC_i*u_i)^2]^{(1/2)}$ = 0.242 → 0.3	ν_R = 131

Figure 26 shows a Pareto chart with each of the independent parameters in the fuel flow calculation. The Pareto chart clearly shows that the largest contributors to the combined uncertainty are the fuel temperature, flowmeter calibration, flowmeter frequency, and fuel density. These are the same parameters that were assumed to be the largest contributors in Section 4.2.1. No reassessment of elemental uncertainties needs to be performed.

4.3.2 Monte Carlo Method

The Taylor's Series method that was used in Table 6 assumed that no significant correlations exist between error sources. This assumption can be tested by using the Monte Carlo method of uncertainty propagation and comparing the results to the Taylor's Series method.

A Monte Carlo uncertainty calculation was performed with 10,000 iterations using the elemental uncertainty values from Table 5 and assuming a normal distribution for each error source. Figure 27 shows the convergence of the standard deviation throughout the simulation. The standard deviation converged to within 1% of the fully converged value after less than 1000 iterations. Figure 28 shows the distribution of the Monte Carlo results. The results are clearly normally distributed.

The converged standard deviation of the Monte Carlo results is 0.122% of reading. Using a coverage factor of 2 for the 95% coverage interval, the expanded uncertainty for fuel flow is then 0.244%, which is almost exactly the same uncertainty result that was obtained using the Taylor's Series method.

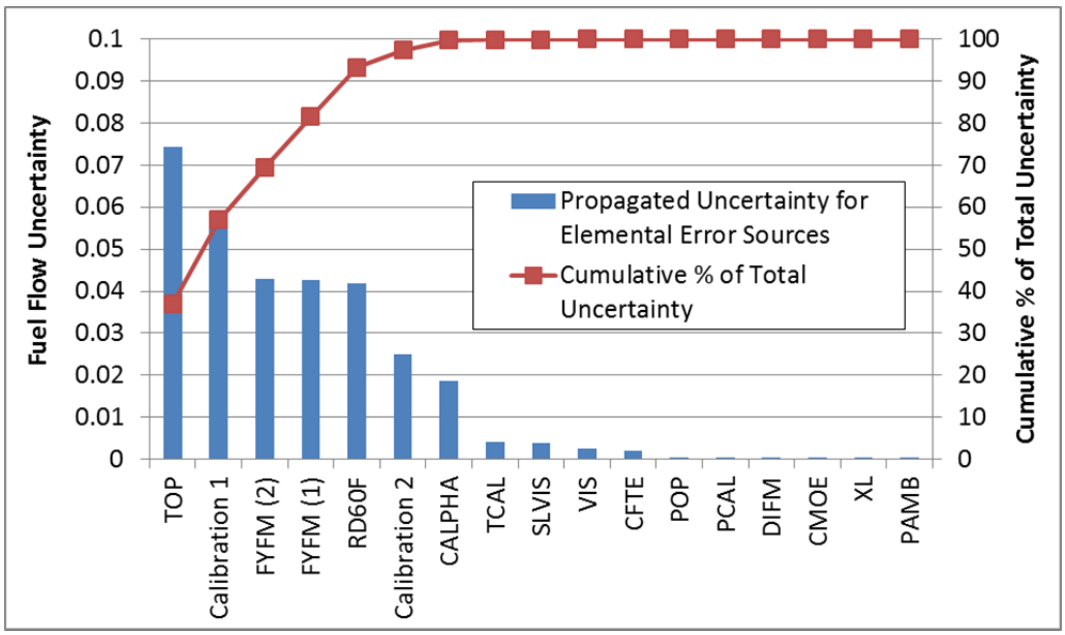

Figure 26. Pareto Chart of Taylor Series Method Uncertainty Calculation

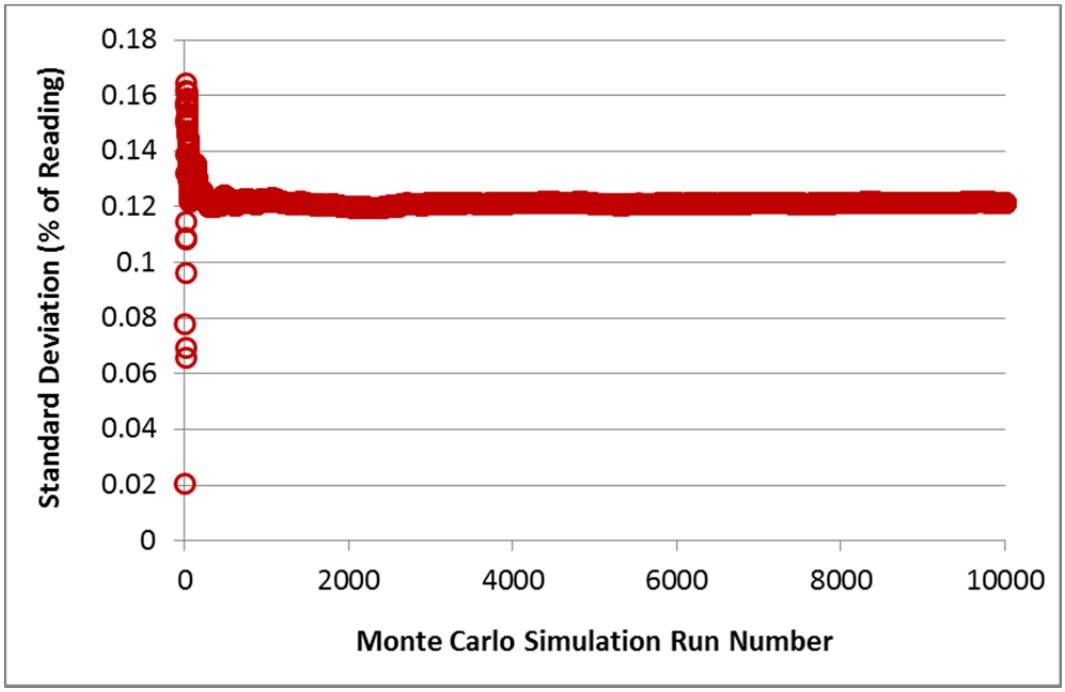

Figure 27. Convergence of Standard Deviation Using Monte Carlo Simulation

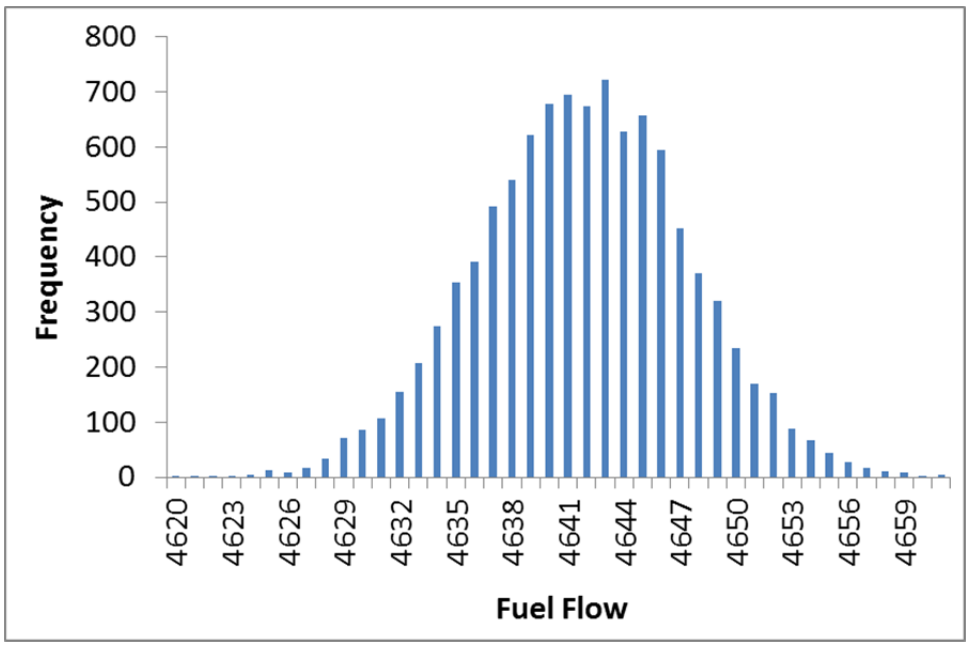

Figure 28. Distribution of Monte Carlo Simulation Results

5.0 CONCLUSIONS

A methodology was presented to derive the fuel flow uncertainty for any given turbine engine test program where the SAE ARP 4990 standard is used to calculate fuel flow. The uncertainty methods presented herein resulted in a combined uncertainty quote that is lower and more statistically defensible than the uncertainty that has historically been quoted for fuel flow at AEDC.

Two uncertainty propagation methods were used to propagate the elemental uncertainties through the fuel flow calculation: the dithering method (a numerical approximation of the Taylor's Series method) and the Monte Carlo method. The two methods resulted in the same value for the combined fuel flow uncertainty. Either of these methods is proposed as a useful way to estimate the fuel flow uncertainty for a test program. It is recommended to use both methods (as often as time and resources allow) in order to validate the results of either method.

The uncertainty analysis showed that four main factors drive the uncertainty: flowmeter frequency, flowmeter calibration, fuel temperature, and relative density constant at the reference temperature. The density input and fuel temperature are used to calculate the operational fuel density and thus have a large effect on the conversion from volumetric flow (measured by the meter) to mass flow. The flowmeter frequency and the flowmeter calibration have a direct 1-to-1 (on a percent basis) impact on the total fuel flow calculation. While the other inputs to the fuel flow calculation do have an effect on the uncertainty, their

effects on the combined fuel flow uncertainty are negligible compared to aforementioned parameters. When performing a detailed uncertainty analysis, it is necessary to validate that the values for all of the inputs are correct, but the majority of the uncertainty analysis should focus on evaluating the elemental uncertainties for frequency, calibration, fuel temperature, and density.

Future work in fuel flow measurement uncertainty should be performed to reduce the uncertainty of the fuel temperature measurement, which is the largest contributor to fuel flow measurement uncertainty. Work could also be performed to create a program with a guided user interface to enable the novice uncertainty analyst to perform Monte Carlo simulations for the purpose of propagating uncertainties.

LIST OF REFERENCES

1. Coleman, Hugh W. and W. Glenn Steele. *Experimentation, Validation, and Uncertainty Analysis for Engineers*. 3rd ed. Hoboken, NJ: Wiley, 2009. Print.
2. Dieck, Ronald H., *Measurement Uncertainty: Methods and Applications*. 4th ed. Research Triangle Park, NC: ISA, 2007.
3. Abernathy, R. B. and Ringhiser, B. "The History and Statistical Development of the New ASME-SAE-AIAA-ISO Measurement Uncertainty Methodology." Presented at AIAA / SAE / ASME / ASEE 21st Joint Propulsion Conference, Monterey, CA. 1985.
4. The American Society of Mechanical Engineers. *Test Uncertainty*. ASME PTC 19.1-2005. New York, NY: ASME, 2005.
5. Taylor, James L. "Establishing Measurement Uncertainty for the Digital Temperature Scanner Using Calibration Data". AEDC-TR-13-P-9. Arnold Air Force Base, TN: Arnold Engineering Development Center, 2013.
6. Abernathy, R. B. et al. and Thompson, Jr., J. W. "Handbook – Uncertainty in Gas Turbine Measurements". AEDC-TR-73-5. Arnold Air Force Base, TN: Arnold Engineering Development Center, 1973.
7. Joint Committee for Guides in Metrology. *Evaluation of Measurement Data — Guide to the Expression of Uncertainty in Measurement.* JCGM 100:2008.
8. SAE International Aerospace Recommended Practice, "Turbine Flowmeter Fuel Flow Calculations". SAE Standard ARP4990. 1997.
9. Joint Committee for Guides in Metrology. *International Vocabulary of Metrology — Basic and General Concepts and Associated Terms (VIM)*. JCGM 200: 2008.

10. National Institute of Standards and Technology. *Guidelines for Evaluating and Expressing the Uncertainty of NIST Measurement Results*. NIST Technical Note 1297. 1994 Edition.
11. Mattingly, Jack D. *Elements of Propulsion: Gas Turbines and Rockets*. Reston, VA: AIAA, 2006.
12. Ku, Harry H. “Notes on the Use of Propagation of Error Formulas”. NBS Report No. 9011. Washington DC: National Bureau of Standards. 1965.
13. Mattingly, George E. “Liquid Flow Measurement: Meters (Part 1)”. May 2005. PowerPoint Presentation.

VITA

Paul A. Wright was born in Vincennes, Indiana in October 1987 to Mr. Roger V. Wright and Mrs. Mary A. Wright. His secondary education was received at Lincoln High School in Vincennes, Indiana. Paul attended Lipscomb University in Nashville, Tennessee and graduated with a Bachelor of Science in Mechanical Engineering with a 3.97 grade point average as the top graduate of his engineering class in 2010. After graduating from Lipscomb University, Paul began work as a turbine engine analysis engineer for Aerospace Testing Alliance, the primary operating contractor for Arnold Engineering Development Complex (AEDC), located on Arnold Air Force Base, Tennessee. In March 2015, Paul transitioned from contractor to civil service employment as a lead test analyst for the aeropropulsion test division at AEDC. Paul enrolled in the graduate program at the University of Tennessee Space Institute in the spring of 2011.